SatCO2

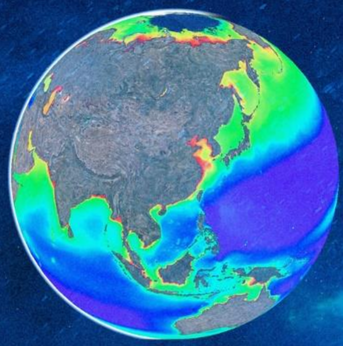

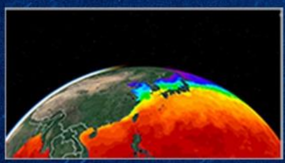

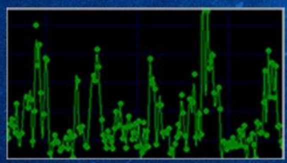

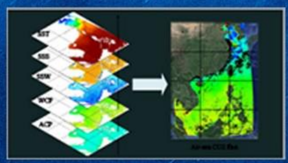

Online analysis SURPORT for multiple sources & time series satellite data

Marine Satellite Data Online Analysis Platform

SatCO2-Pro. V1.0

User Manual

State Key Laboratory of Satellite Ocean Environment Dynamics
Second Institute of Oceanography, MNR
Zhejiang Provincial Key Laboratory of Geographic Information Systems
Department of Earth Sciences, Zhejiang University

November, 2018

Notices

1. SatCO2 platform and its data are free. The goal of the platform is to promote marine satellite data sharing and multidisciplinary application. All images and data available on the SatCO2 platform are for research and educational use only. When using SatCO2 data in a research or education project, please include the citation (SatCO2 platform as well as the relevant algorithms involved and the providers of the original data). For more information, please refer to the website: www.SatCO2.com.
2. The advantages of satellite data include long time series and wide spatial coverage. Some successful algorithms validated in some regions may need further validation when extending to a larger region or longer time period. SatCO2 platform provides free consulting services regarding data and technical issues; however, the platform is not responsible for improper use of the data in research or application.
3. SatCO2 needs to be installed and operated on user's own computer. If the computer does not have discrete graphics card, the system may run but some functions are not available (for example, in situ data display and symbolization), or the entire system may not run.

   How to check whether your computer is installed with discrete graphics card:

   1) Right-click "My computer/Computer" and left-click "Properties."

   2) Left-click "Device manager."

   3) Left-click "Display adapters," if it shows "AMD" or "NVIDIA," then, it has discrete graphics card. If it shows only "Intel," it does not have discrete graphics card.
4. For high-resolution display, please adjust the display zoom percentage to 100% for user experience.

   How to adjust the display scale:

   1) Right-click in the blank area of the desktop and click display Settings.

   2) Adjust the display zoom percentage of the size of the text to 100%.

Outline

1 Overview of SatCO2 platform

SatCO2 is a marine satellite data online analysis platform, formerly known as the satellite-based marine carbon monitoring and analysis system, hereinafter referred to as the "SatCO2 platform." It is a platform that can simultaneously fulfill visualization and project scientific calculations of multiple-sources satellite data, *in situ* data, and modelling products on a three-dimensional virtual Earth. It is free to the public, to promote sharing and multidisciplinary application of marine investigation data.

The SatCO2 platform was jointly developed by the State Key Laboratory of Satellite Ocean Environment Dynamics of the Second Institute of Oceanography of the Ministry of Natural Resource (SOED/SIO/MNR) and Zhejiang Provincial Key Laboratory of Geographic Information System of Zhejiang University (GISLAB/ZJU). The SatCO2 platform has two components: online database and client software. Users can download the SatCO2 client software for installation and usage. The online services of long time series and multi-source satellite data are provided by the SOED/SIO. A user can conveniently assess the online data from the SOED through SatCO2 system for online visual analysis, and to use the system for comprehensive analysis based the multi-source satellite data and in situ data on user’s own computer.

The major functions of the SatCO2 platform are summarized as follows:

1) Online access of satellite remote sensing data;

2) 3D Earth visualization and scientific computation;

3) Analysis and evaluation of multi-source (satellite, in situ, and model) data;

4) User-defined algorithms and product generation;

5) Calculation and evaluation of ocean carbon flux;

6) Easy integration of professional modules.

1.1 SatCO2 Main Functions

SatCO2 V1.0 software consists of nine main menu items in total, namely, Load Data, View Image, Data Analysis, User-define Algorithm, Comparison Analysis, Budget Calculation, Expanded Apps, and Help, as detailed below.

(1) Load Data

Data loading at the database center: connect with the SOED data center through SatCO2 client software to realize the query and retrieval of satellite data, in situ data, and modeling products shared in the database, and display them in 3D geospheres. The loaded data can be downloaded by right-clicking the data layer list window and exported in the format of .tif.

Local data loading: SatCO2 software supports users’ local satellite and in situ data loading and online analysis. Currently supported formats are .tif, .hdf, .netcdf, and .csv.

(2) Image Display

Image display allows the user to load data and display them in 3D geospheres. The user can customize the image display mode, including: 1) customize the colorbar of satellite data; 2) overlay display on different layers and set transparency; 3) 3D spherical view and image roaming flight; and 4) measure spatial geographic information of selected points, lines, and surface areas.

(3) Data Analysis

The user can select, analyze, and save the data of active layer in different ways of selected points, lines, and surface areas. The user can also search and select the long time series data in the online database by setting different time ranges, and carry out analysis on the points, lines, and areas of interest using the long time series data. System also provides animation playback function of continuous observation satellite product.

(4) User-define Algorithms

1) The user can use the data from online database or data in user’s own computer to generate new satellite products through convenient operation of mouse click and input algorithm formula, and conduct various visual analysis using SatCO2 software. 2) Gridding calculation of in situ or satellite data. 3) Perform data filtering, interest area extraction and data classification for satellite products. 4) Select satellite data in the database, generate custom thematic diagrams, and export them.

(5) Comparison Analysis

Current version provides two functions. 1) Users can use imported in situ data to verify the accuracy of matched satellite products, and obtain scatter diagram and statistical comparison results. 2) Compare two satellite images for the same region.

(6) Budget Calculation

The software provides calculations of air-sea CO2 flux. 1) Air-sea CO2 flux can be calculated using satellite data with system default algorithm or custom algorithm. 2) Air-sea CO2 flux can also be calculated based on in situ data and some matched-up satellite data if some parameters are unavailable from the field measurement, such as wind speed or air CO2. 3) Estimate of carbon budget can be obtained based on air-sea CO2 flux products, via area integral of the interest area.

(7) Theme Application (Expanded Apps)

This part is the thematic functional modules for specific application. The current version only integrates the satellite identification module of harmful algae bloom. More application modules will be integrated into updated version.

(8) Help

This part includes user manual download, update check, source of base map, language switching, etc.

1.2 System Requirements

Requirements	Recommended configuration	Minimum configuration
OS	64-bit Windows 7	32-bit Windows 7/8/10
Processor	Intel Core i5 3470	Intel Core 2 Quad CPU Q6600
Memory	8 GB	4 GB
Hard disk	10 GB	10 GB
Video card*	NVIDIA GTX 660	NVIDIA 9800 GT
Network bandwidth	10 MB	4 MB

[1] SatCO2 needs to be installed and operated on user’s own computer. If the computer does not have discrete graphics card, the software may run but some functions are not available (for example, in sit data display and symbolization), or the entire software may not work.

How to check whether your computer is installed with discrete graphics card:

1) Right-click "My computer/Computer" and left-click "Properties."

2) Left-click "Device manager."

3) Left-click “Display adapters.” If it shows “AMD” or “NVIDIA,” then it has discrete graphics card. If showed only “Intel,” it doesn’t have discrete graphics card.

[2] For a high-resolution display, please adjust the display zoom percentage to 100%.

How to adjust the display scale:

1) Right-click in a blank area of the desktop and click display Settings.

2) Adjust the display zoom percentage of the size of the text to 100%.

1.3 SatCO2 Installation

Please confirm whether the system software and hardware meet the minimum configuration requirements before installation.

Run the system installation package "SatCO2.exe." The installation prompt wizard appears. During installation, you will be prompted to select the installation directory. Please select the non-system packing directory for installation, and make sure that the available disk space is greater than 300 MB. Once the program is installed, you can start the software by double-clicking the desktop shortcut ("SatCO2").

2 Operation Instruction

2.1 Main Screen

The main interface of SatCO2 system is shown in Figure 2-1. The home screen consists of six parts in the order of annotated numbers as follows: 1. Menu bar; 2. Target layer; 3. Layer control panel; 4. Display window; 5. Product color-bar; and 6. Output window (showing results of query, analysis, and calculation).

1) Menu bar: main function operation button.

2) Target layer: select the target image to be processed from the currently loaded image. In general, the system defaults to the latest loaded image (the top layer in the layer control panel) as the target layer.

3) Layer control panel: display the layer data that have been loaded into the 3D geosphere. Left-click to display/hide the layer, right-click to set the top/remove the layer, and double-click layer name to zoom the view to default if it is too large or too small.

4) Display window: layer display and the main window for operation. Users can rotate the geosphere using the mouse.

5) Product color-bar: set the corresponding color label for the currently selected layer. It can be set manually to display or be closed.

6) Output window: output query/calculation results.

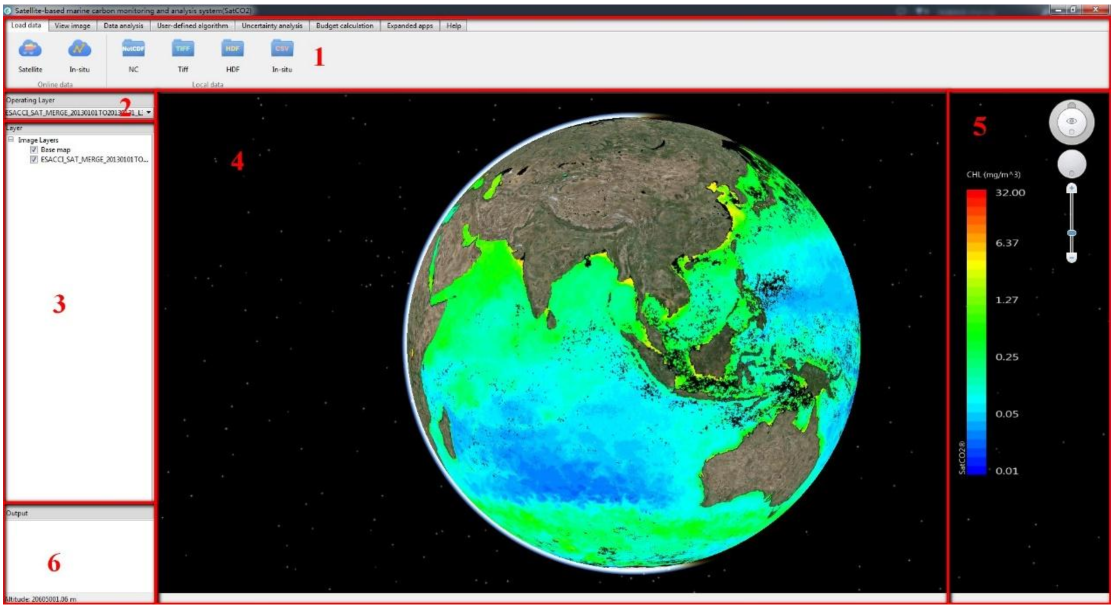

Figure 2-1. Main screen

2.2 Load Data

The “Load Data” tab is designed to load the database or user’s own data to the display window (Figure 2-2).

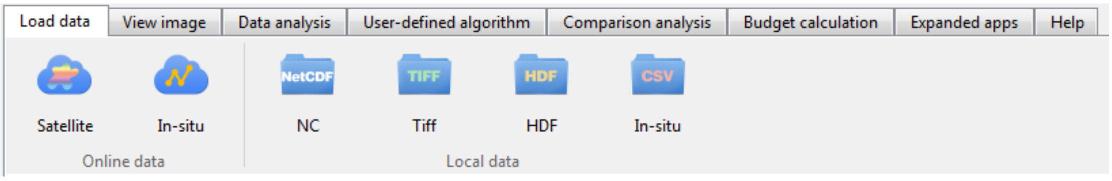

Figure 2-2. Load data tab

2.2.1 Load SOED online database

2.2.1.1 Satellite database

Click the “satellite” button in the SOED online database, and the satellite product query dialog box will pop up (Figure 2-3).

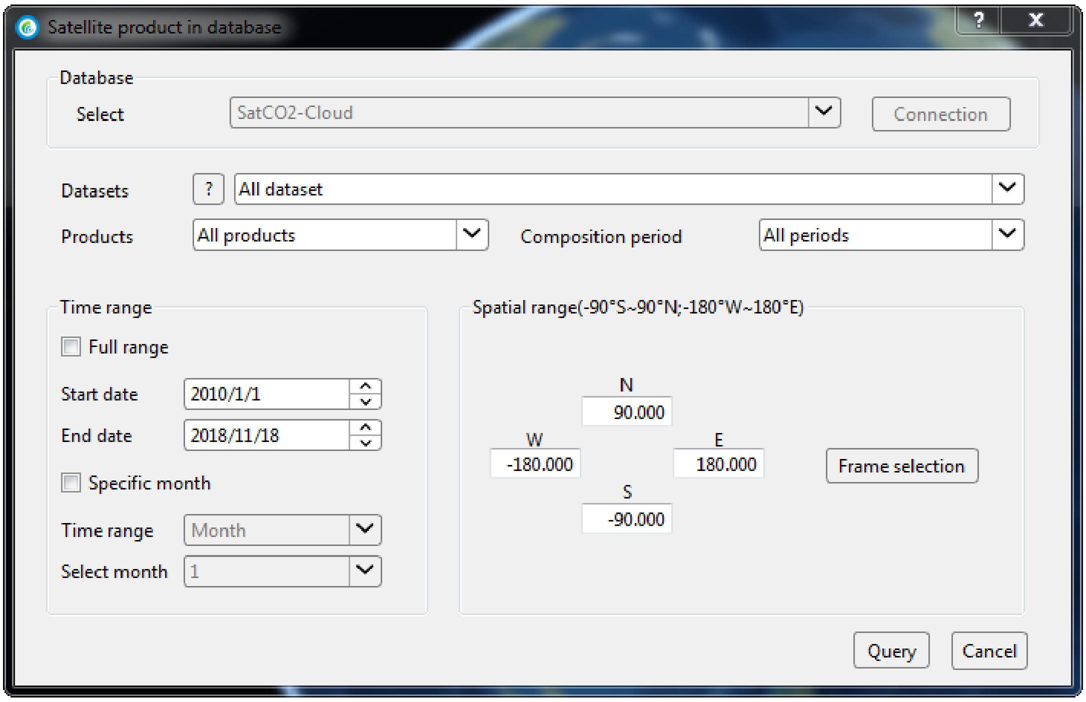

Figure 2-3. Satellite product in database dialog

Users can set the corresponding “data sets,” “product type,” “composition period,” “time range,” and “spatial range” for query. Query result is shown in Figure 2-4.

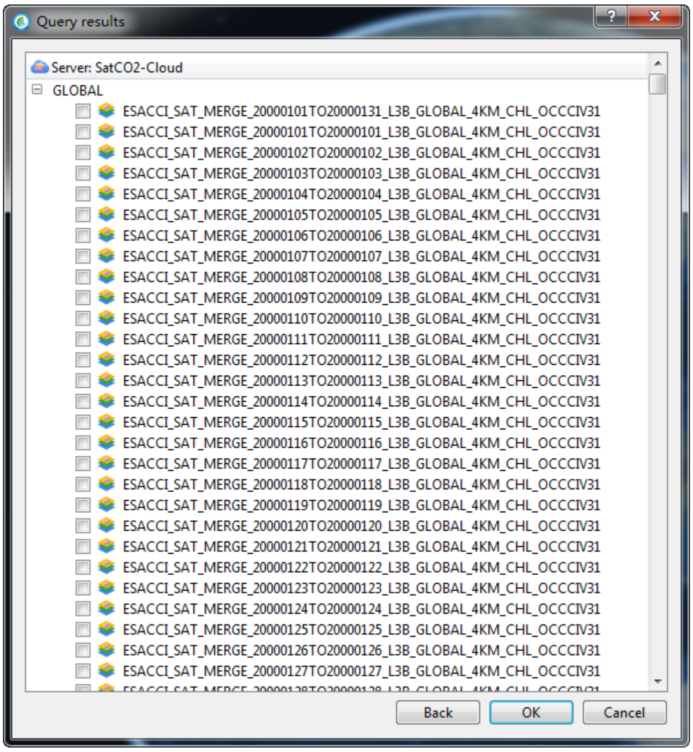

Figure 2-4. Query result (The system does not provide "full selection" function, and the load time is related to the number of selected products.)

In the product “Query result” dialog, select the desired product and determine if the selected product is loaded directly to the 3D geosphere. Click the "OK" button, and the selected product will be loaded as a layer into the 3D display window (Figure 2-5). The loaded product is displayed in the left layer control panel window, and the user can operate the layer display order in the drop-down box of the target layer, or right-click on the related layer name for further operations.

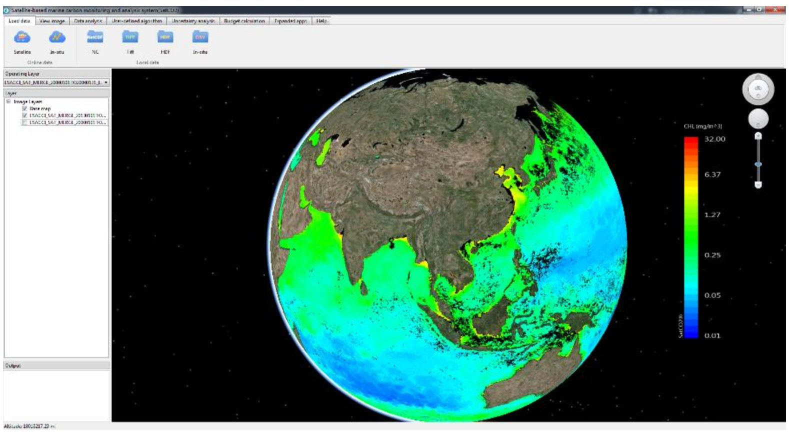

Figure 2-5. Loaded satellite product

2.2.1.2 In situ database

Click the button of "In-situ," and the dialog box of in situ data query will pop up (Figure 2-6). For the time being, only the global underway data set of the CDIAC database is included.

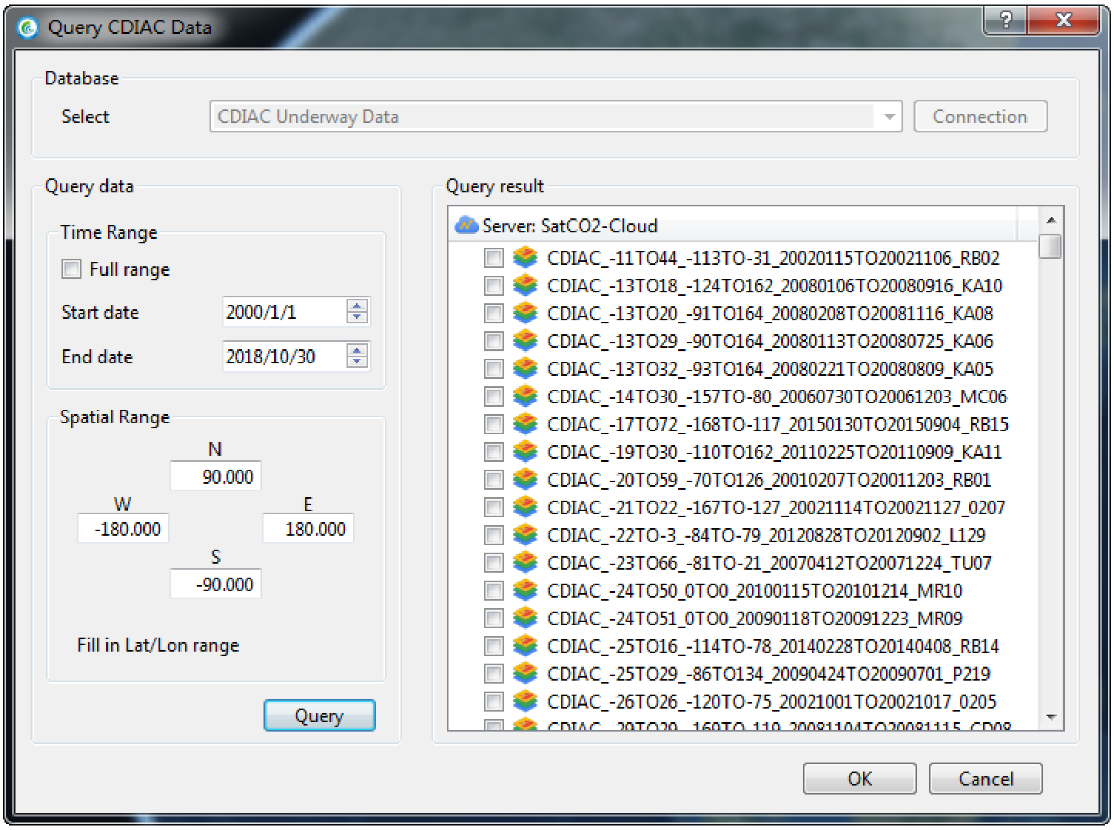

Figure 2-6. In situ data query dialog

2.2.2 Load local data

2.2.2.1 NetCDF data

Click the NetCDF button to import the .nc format satellite data stored in user's own computer. The user can select the sub-dataset of .nc file that needs to be loaded (Figure 2-7), click "OK" to load it into 3D geosphere. Result is shown in Figure 2-8.

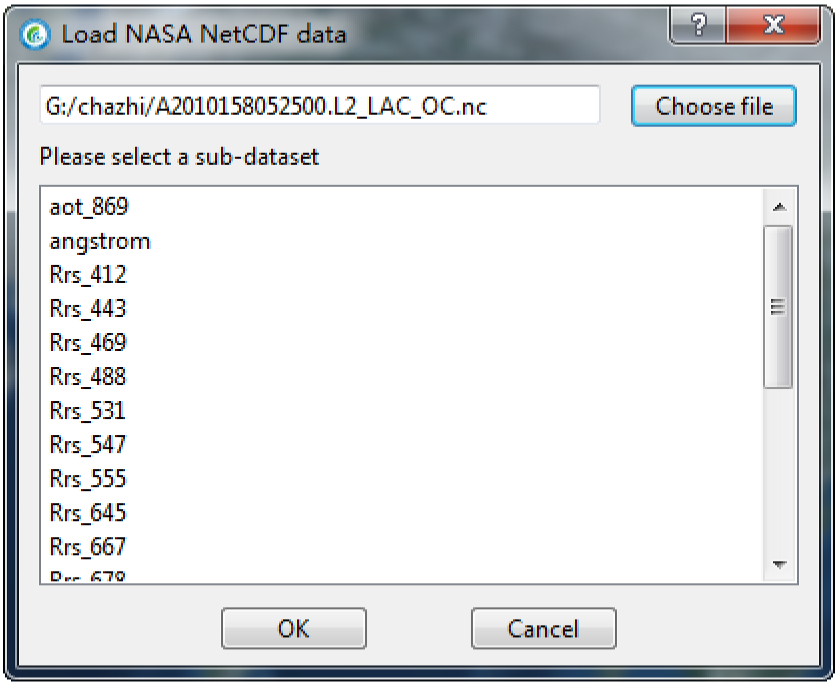

Figure 2-7. Load NetCDF data

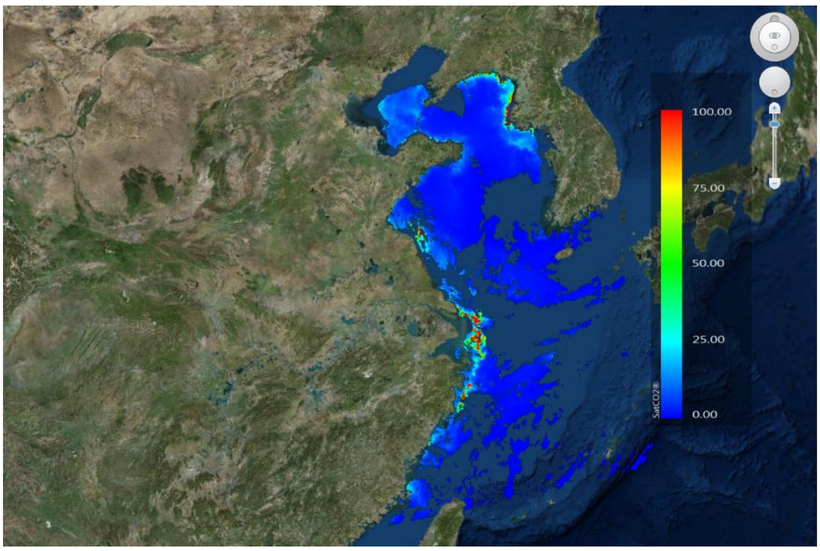

Figure 2-8. NetCDF data loaded

2.2.2.2 HDF data

Users can also use SatCO2 software to open satellite data in .hdf format. However, users are required to provide the latitude and longitude ranges of the satellite data, as well as invalid value identification. (Other software can be used to obtain the above information such as the HDF explorer.)

After clicking the “HDF” button, a dialog box will pop up (Figure 2-9). Select the local HDF data to open and click "Next." After filling in the information such as “spatial range,” “No value,” “parameters,” etc. (Figure 2-10), the HDF data can be loaded into the 3D geosphere (Figure 2-11).

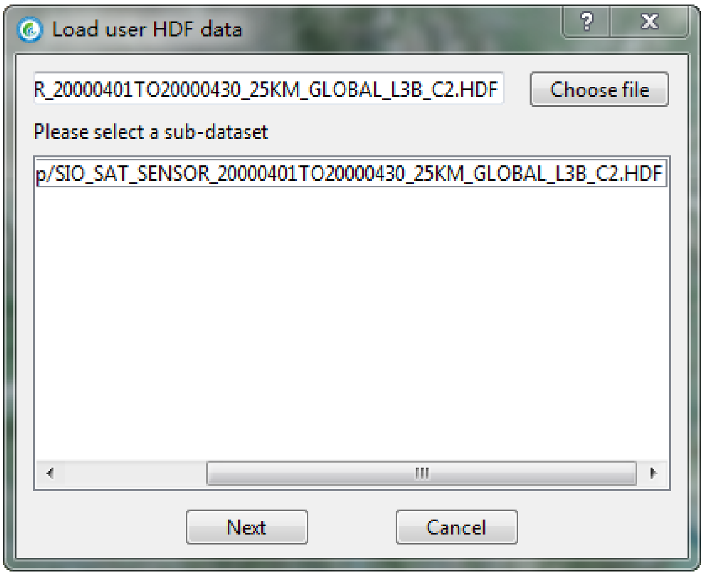

Figure 2-9. Load user HDF data dialog

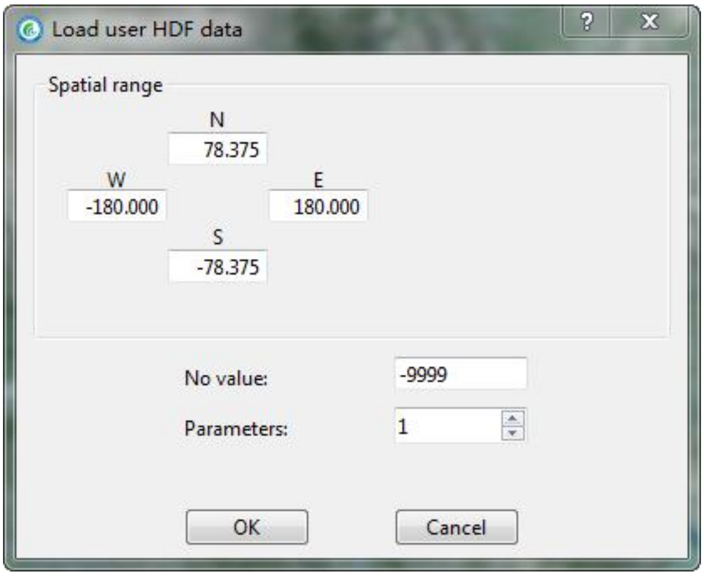

Figure 2-10. Fill in the dialog box for information

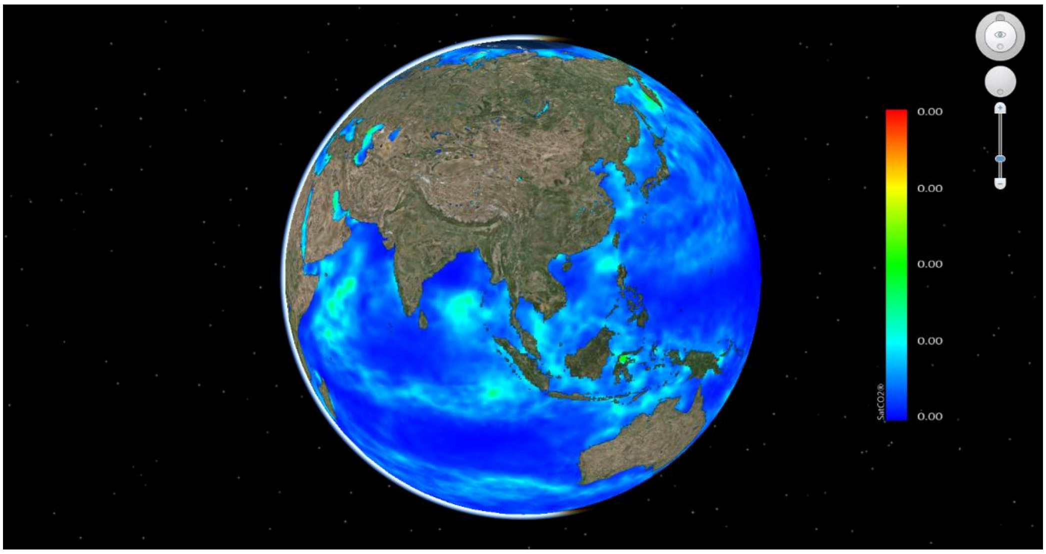

Figure 2-11. HDF data loaded

2.2.2.3 TIFF data

Click the “TIFF” button and select the local .tif data to load into the 3D geosphere.

2.2.2.4 In situ data

After clicking the "In-situ" button, the pop-up dialog box is used to import the local in situ data in .csv format (Figure 2-12).

The in situ data shall be pasted in the CSV table according to certain rules. Click the button of “generate template” in the window, and the .csv template can be exported to the local directory. The exported template is shown in Figure 2-13, where columns A to D are listed as required information (longitude, latitude, date, hour) and cannot be deleted. The user adds other parameters’ information in the follow-up columns. After pasting the corresponding data in the template and saving it, click the “load data” button to load it into the 3D geosphere (Figure 2-14).

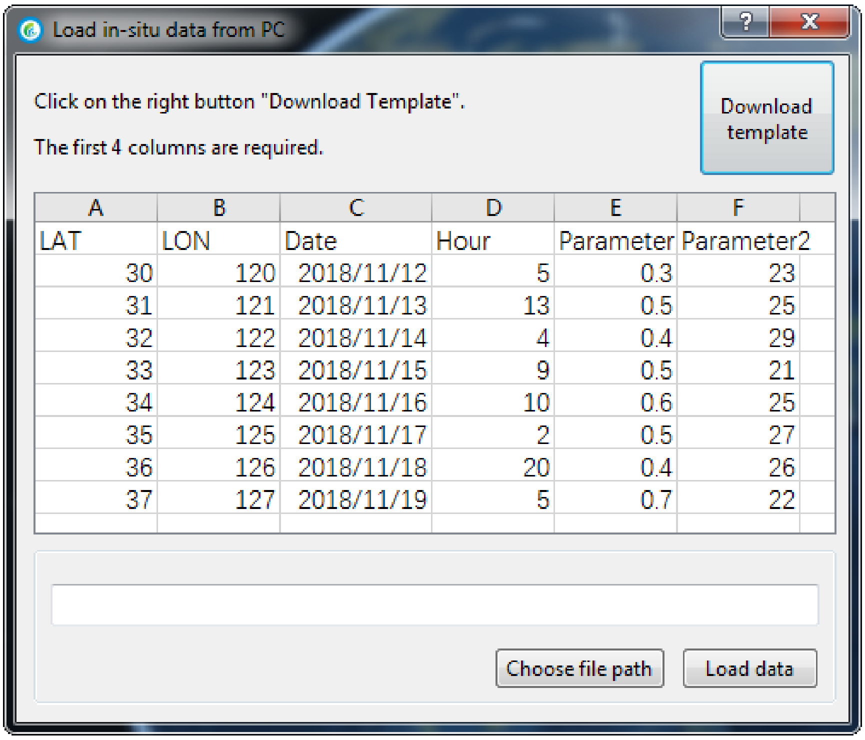

Figure 2-12. Load local in situ data dialog

A	B	C	D	E
LAT	LON	Date	Hour	Parameter1

Figure 2-13. In situ data template

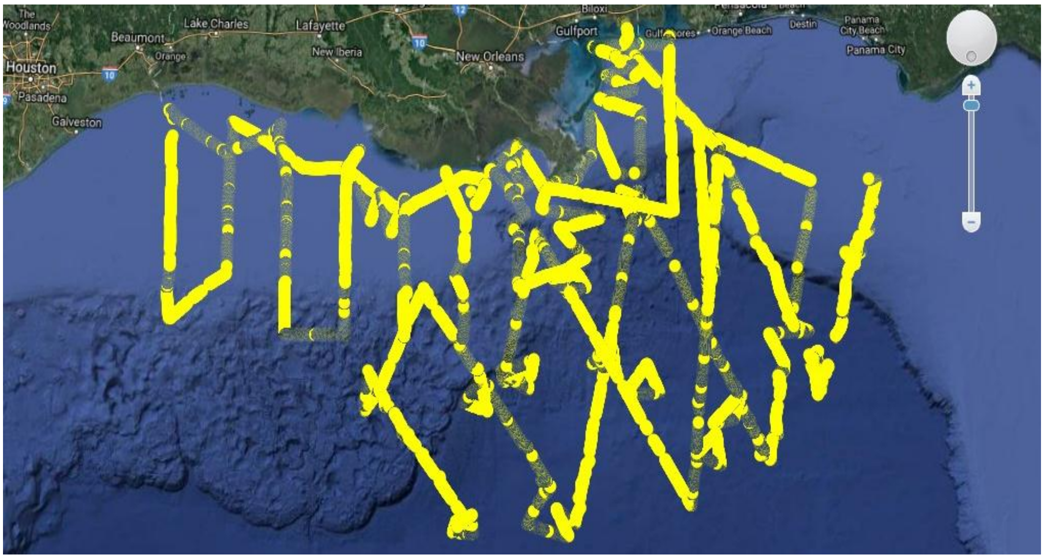

Figure 2-14. In situ data loaded

2.3 View Image

The main display window is a 3D view centered on a 3D geosphere. It provides functions such as data loading, comparison, display, editing, and scene simulation.

The “View image” tab includes four modules: “image adjustment,” “spatial measurement,” “navigation,” and “view” for adjustment, navigation, and browsing of the current 3D geosphere (Figure 2-15).

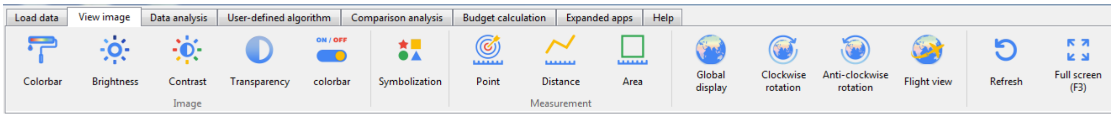

Figure 2-15. View image tab

2.3.1 Image adjustment

The “image adjustment” module includes “colorbar,” “brightness,” “contrast,” “transparency,” and “color bar” switch buttons.

Click “colorbar” switch to display/hide the product colorbar of the selected target image. The colorbar includes product type, units, and stretch ribbon (Figure 2-16).

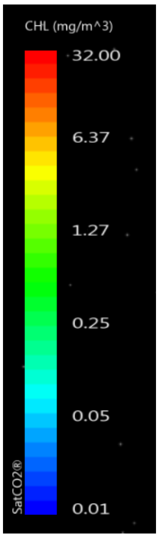

Figure 2-16. Colorbar

The “colorbar” is the render method of image display mainly for raster data. Click "colorbar” " to pop up the raster data rendering dialog box (Figure 2-17). The raster data rendering dialog box includes two tabs: classified rendering and stretch rendering.

In “classified rendering,” the user can select the default product color label template in the system through the pull-down box to render the layer (Figure 2-17). The user can also click user-defined class to render the layer.

Click "stretch render," and the stretch render tab will pop up (Figure 2-18). User completes the setting of the stretching colorbar by selecting the color band (reversible) and stretching type (such as standard deviation, maximum/minimum values).

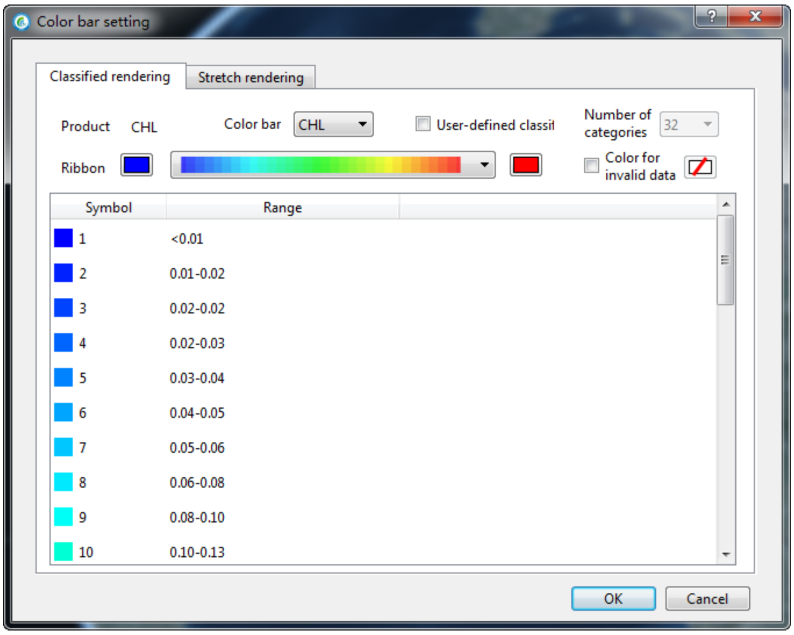

Figure 2-17. Colorbar setting dialog

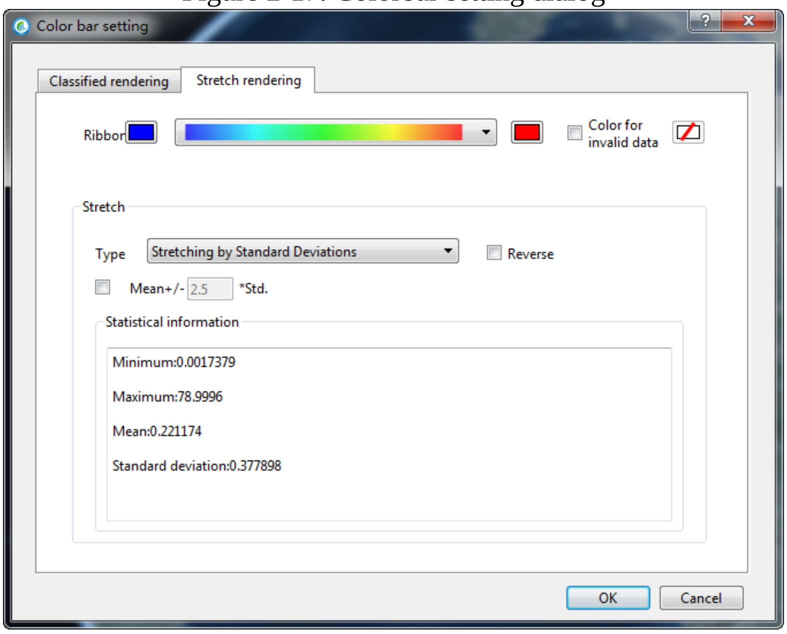

Figure 2-18. Stretch rendering dialog

2.3.2 Symbolization

The symbolization function is mainly aimed at the in situ data, such as station measurements or the underway data. Select the in situ data that need to be symbolized. And click the “symbolization” button to perform the symbolization operation on all elements of the in situ data (Figure 2-19, 2-20). The symbolic result is shown in Figure 2-21. Discrete graphics card is required for using this function.

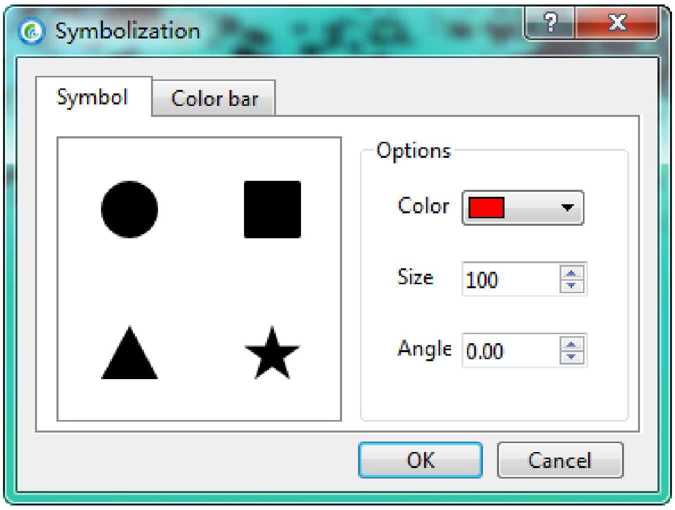

Figure 2-19. Symbolization dialog

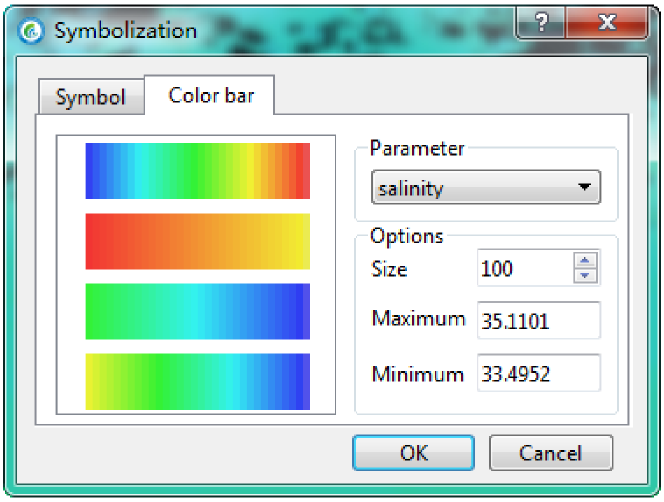

Figure 2-20. Color bar for symbolization in situ data

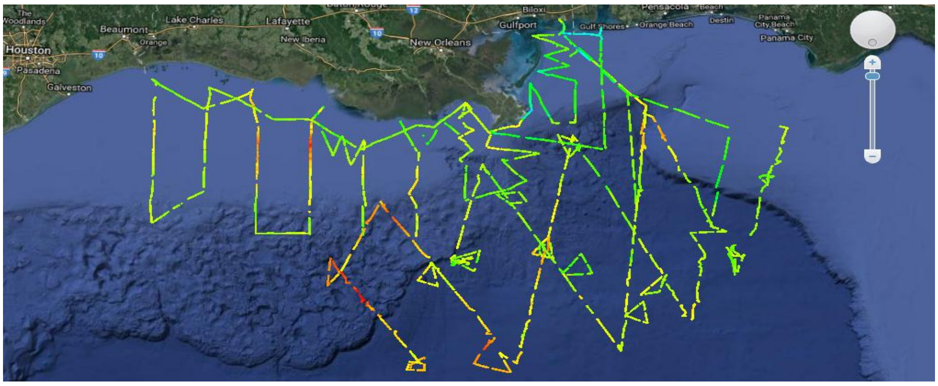

Figure 2-21. Stretching results of symbolized underway salinity data

2.3.3 Spatial measurement

Spatial measurement module includes “point measurement,” “distance measurement,” and “area measurement.”

Click “point measurement” button, and then click on the geosphere interested target. The latitude and longitude coordinates can be obtained (Figure 2-22).

Output

Longitude: -163.814°
Latitude: -0.726234°

Figure 2-22. Point measurement output

Click the “distance measurement” button, and draw lines on the geosphere to get the distance. The result is shown in Figure 2-23.

Output

Total length: 1598.51km

Figure 2-23. Distance measurement output

Click “area measurement” button, choose points on the geosphere in turn to draw a polygon, double-left-click to close the polygon. The system will measure the area of the region the polygon contains, and the result is shown in Figure 2-24.

Output

Area: 429199 Square kilometer

Figure 2-24. Area measurement output

2.3.4 Navigation

The navigation module provides the function of "global display," "clockwise rotation," "anti-clockwise rotation," and "flight view."

Global display: scale the 3D geosphere to the global display.

Clockwise/anti-clockwise rotation: rotate the 3D geosphere clockwise or counter-clockwise.

Flight view: click multiple points on the geosphere to complete the custom path by the left mouse button. Select the flight time and height to browse.

2.3.5 View

View module includes “refresh” and “full screen” functions.

Refresh: Refresh all the loaded layers to clear the cache.

Full screen: full-screen display(hot key is [F3]). Press [Esc] to exit the full screen.

2.4 Data Analysis

The data analysis tab provides the function of making analysis on the points, lines, or areas of interest in the target image. One example is shown in Figure 2-25.

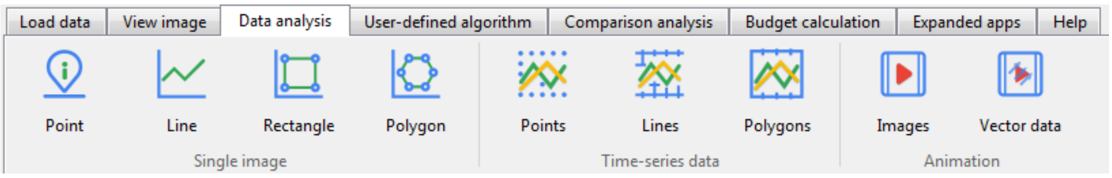

Figure 2-25. Data analysis tab

2.4.1 Point

Click the "point" button, and the query dialog box will pop up (Figure 2-26). The query mode has three types: 1) click directly on the image to select points of interest; 2) enter the longitude and latitude information of interested points in the dialog box; and 3) import a file with multiple points of latitude and longitude information from user's local computer, such as the stations' positions or underway information.

Click "import" to load the .txt format file of lon/lat information recorded in "longitude, latitude" format. Click "export," and export the information of the selected point in batches (Figure 2-27). The user can select the .txt file exported from the previous layer, and read the information of the same latitude and longitude points from the current layer.

This function only queries the spatially matching information in a single layer. If the user needs to match multiple satellite data files from different times, use the "comparison analysis" menu.

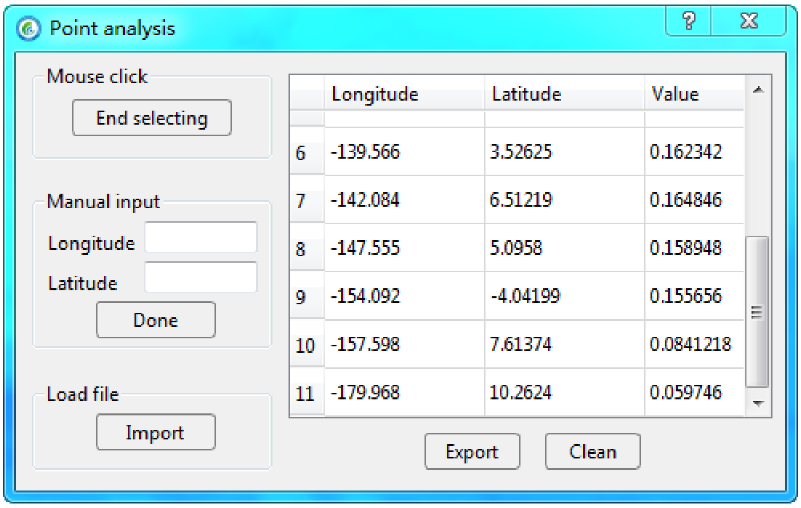

Figure 2-26. Point analysis dialog

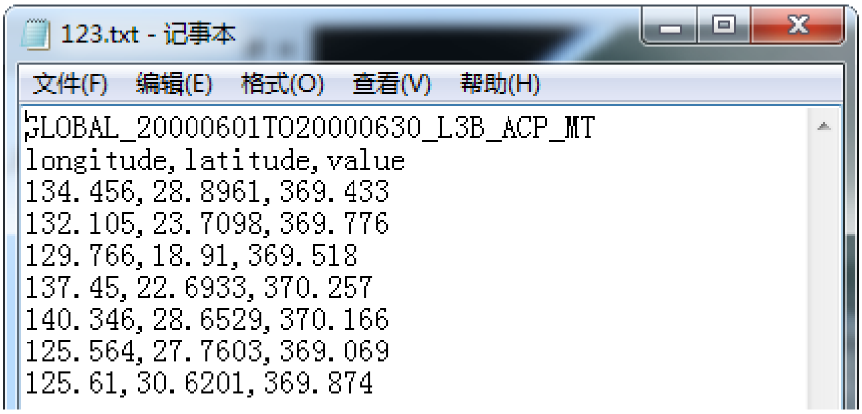

Figure 2-27. Export .txt file

2.4.2 Line

Click the "line" button to draw a polygonal line on the selected target image (Figure 2-28). The software uses the grid data along the polygonal line to generate a polygonal line graph, and calculates the statistical information (maximum, minimum, average, and standard deviation) of all grid points on the polygonal line. There are two categories of results: one with the x-axis of longitude through the polygonal line (Figure 2-29), and the other with the x-axis of distance between the points on the polygonal line and the starting point (Figure 2-30).

In addition, you can select other layers in the drop-down box and click the "analysis" button to output the analysis results of the same polygonal line position in other satellite data (Figure 2-31).

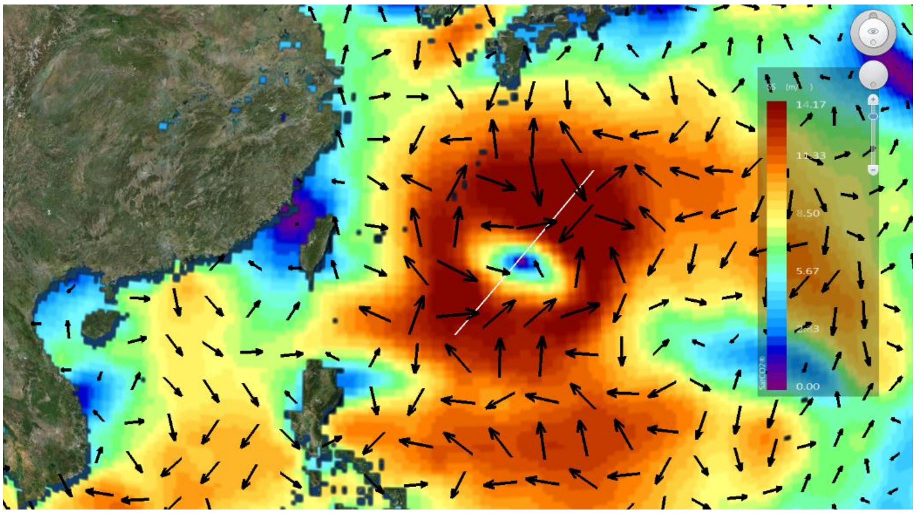

Figure 2-28. The wind speed and direction image of Typhoon Morakot, the eighth typhoon of 2009, with a resolution of 25 km, on August 5, from the data set of CCMP wind field. The color represents the 10-m wind speed over the sea surface, and the arrow represents the wind direction. The white line is the selected line for line analysis.

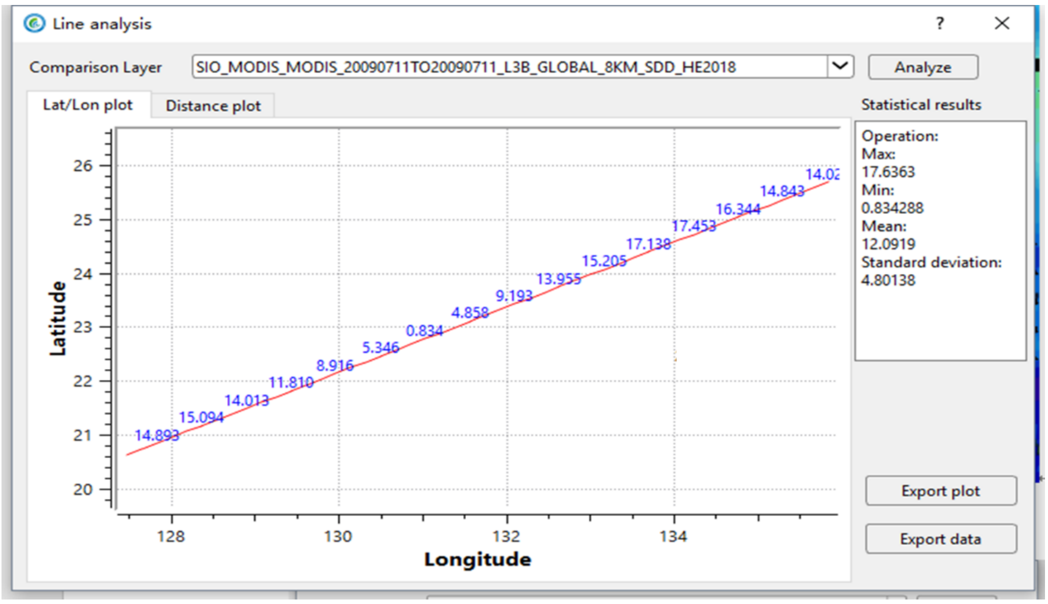

Figure 2-29. The longitude/latitude plot obtained by line analysis. The x-axis is the longitude of the polygonal line, and the y-axis is the latitude. The right column is the basic information of all grid points on the polygonal line. It shows that the maximum wind speed on the polygonal line is 17.6363 m/s, the minimum wind speed is 0.834288 m/s, and the average wind speed is 12.0919 m/s. The spatial variation of wind speed can be clearly seen by the latitude/longitude plot.

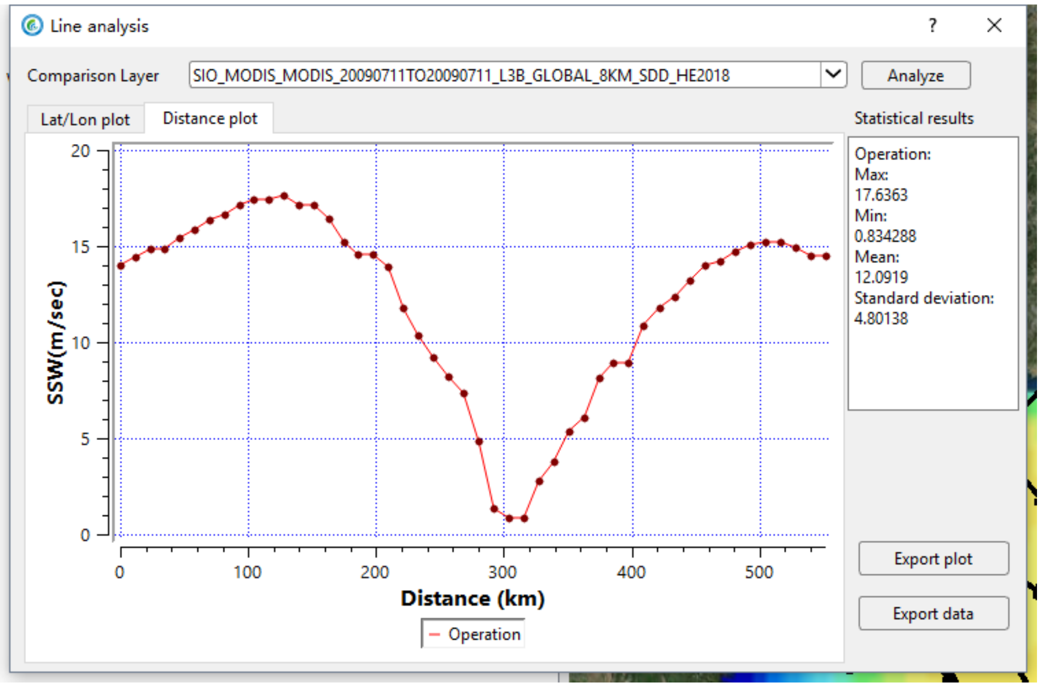

Figure 2-30. The distance plot obtained by line analysis. The x-axis is the distance between the points on the polygonal line and the starting point, and the y-axis is the wind speed. The gradual increase of wind speed from the typhoon eye to the periphery is clearly shown by the distance plot.

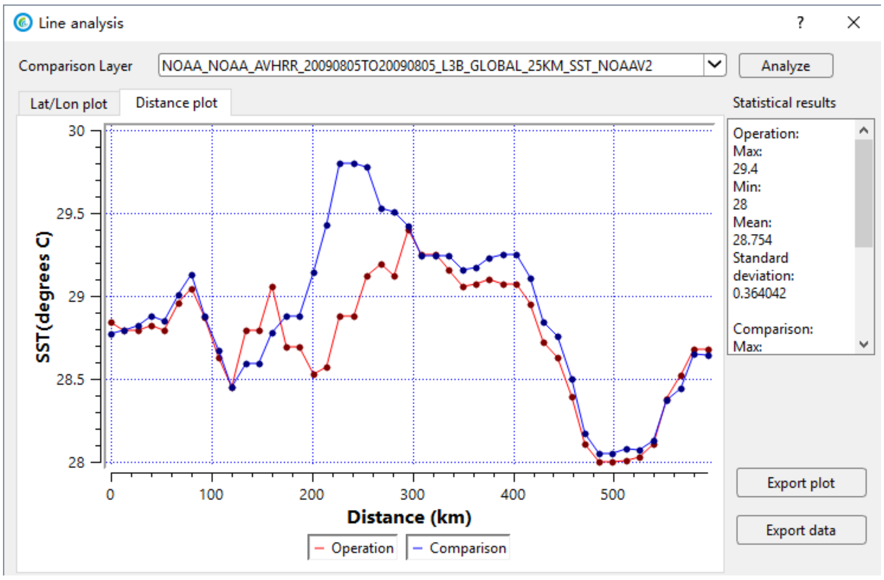

Figure 2-31. A comparison plot obtained by line analysis. The x-axis is the distance between the points on the polygonal line and the starting point, and the y-axis is the sea surface temperature (SST). The blue line represents SST of the grid points selected on August 5, and the red line represents the SST of the grid points on August 6. This comparison shows the SST decreased after the typhoon. By using the function of layer comparison, users can see the change of the selected polygonal line in different satellite images. It can be used to compare the variation of a parameter in the region of interest at different times, or show the variation of different parameters in the region of interest at the same time.

2.4.3 Rectangle

Click the “rectangle” button and drag the mouse to draw a rectangle on the selected image (Figure 2-32). The system will conduct statistical analysis on the effective grid data contained in the rectangle. The histogram of the selected region is generated, and results such as maximum, minimum, and standard difference are outputs (Figure 2-33).

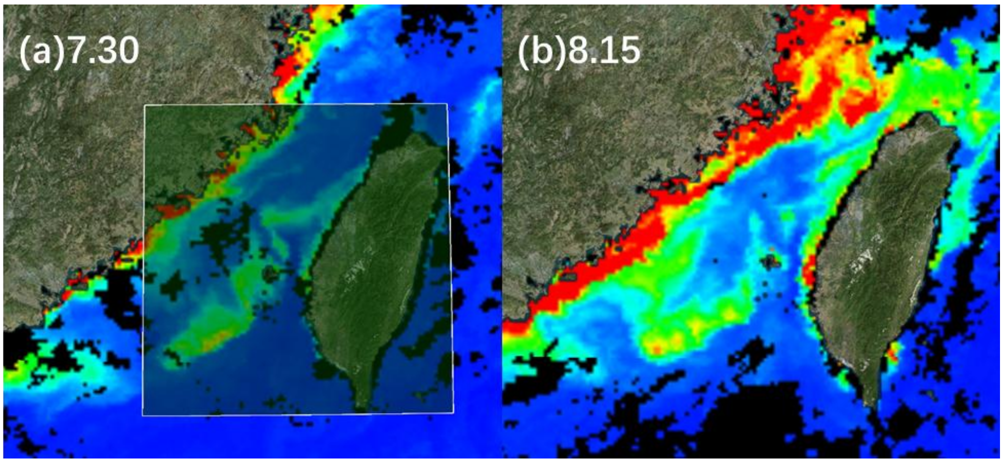

Figure 2-32. Image of sea water transparency at 8-km resolution in the Taiwan Strait (a) before Typhoon Morakot passing through (on July 11) and (b) after Typhoon Morakot passing through (August 14). The green transparent rectangle represents the area selected for the rectangle analysis. After He et al. (2015). [Satellite views of the episodic terrestrial material transport to the southern Okinawa Trough driven by typhoon. Journal of Geophysical Research Oceans, 119(7), 4490-4504.]

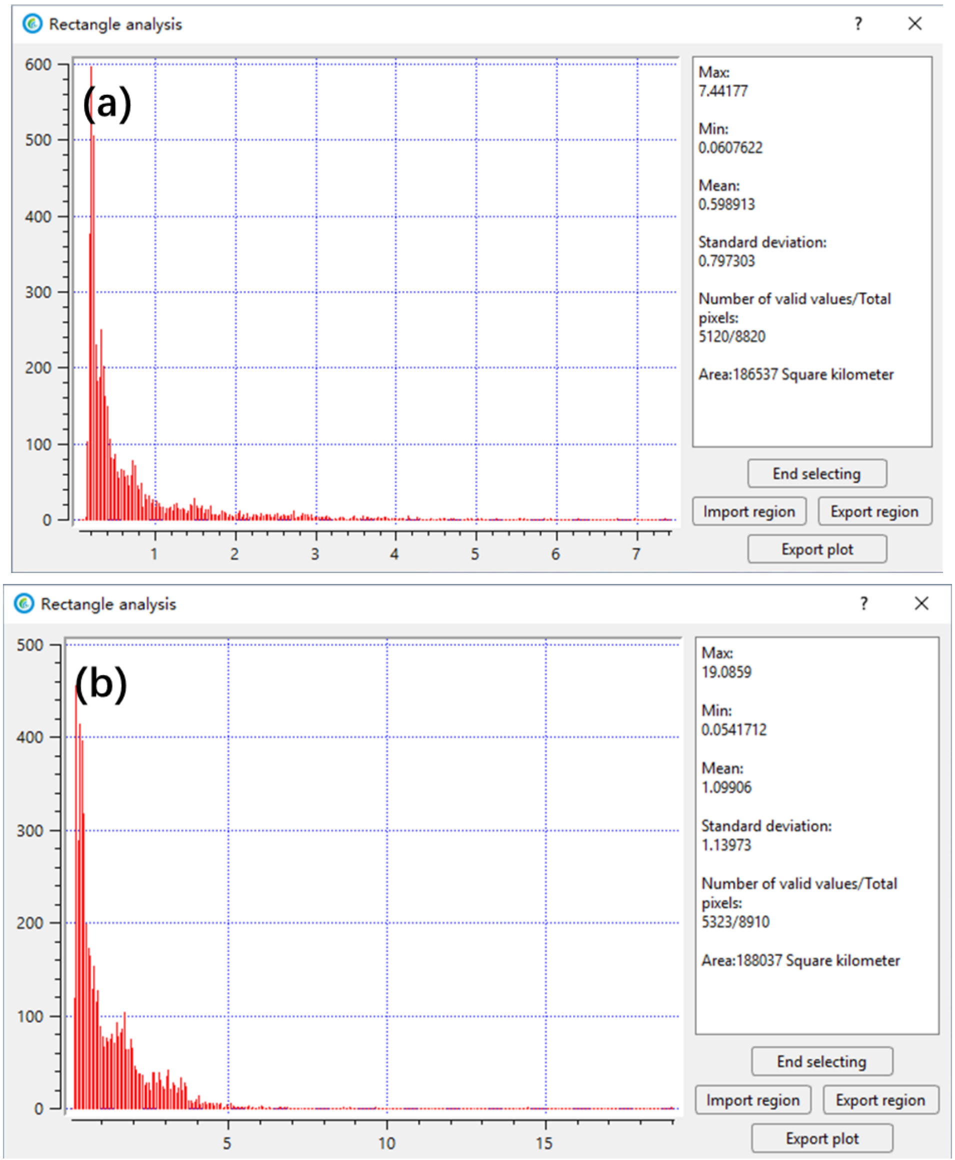

Figure 2-33. Rectangular analysis results. Statistical results show that the average chlorophyll concentration was 0.599 mg/m^3 on July 30 (a) and was 1.099 mg/m^3 on August 15 (b). As can be seen from the histogram and mean value, the chlorophyll concentration in the Taiwan Strait was higher after the typhoon passing through.

2.4.4 Polygon

Click the “polygon button,” select the points to draw polygons in the target image, and double-click the left button to close the polygon automatically (Figure 2-34).

For the area corresponding to the irregular coastline, users can import the .txt file containing latitude and longitude coordinates of polygon corner themselves.

The software can generate histogram of the selected region and output statistical results, such as maximum, minimum, average, and standard deviation (Figure 2-35).

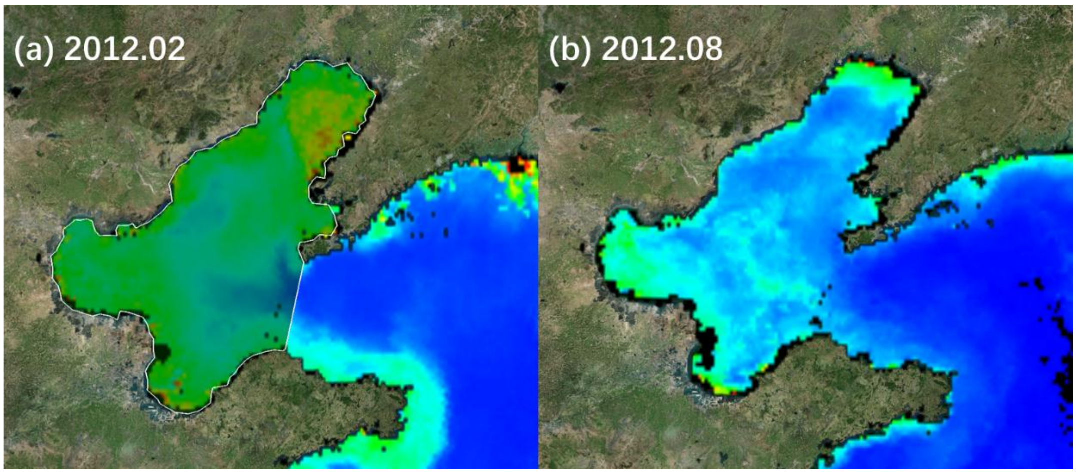

Figure 2-34. Monthly average chlorophyll concentration of 4-km resolution in the Bohai Sea in February 2012 (a), and August 2012 (b), obtained from ESACCI data set. The green transparent polygon is imported by a pre-made .txt file containing Bohai coastlines.

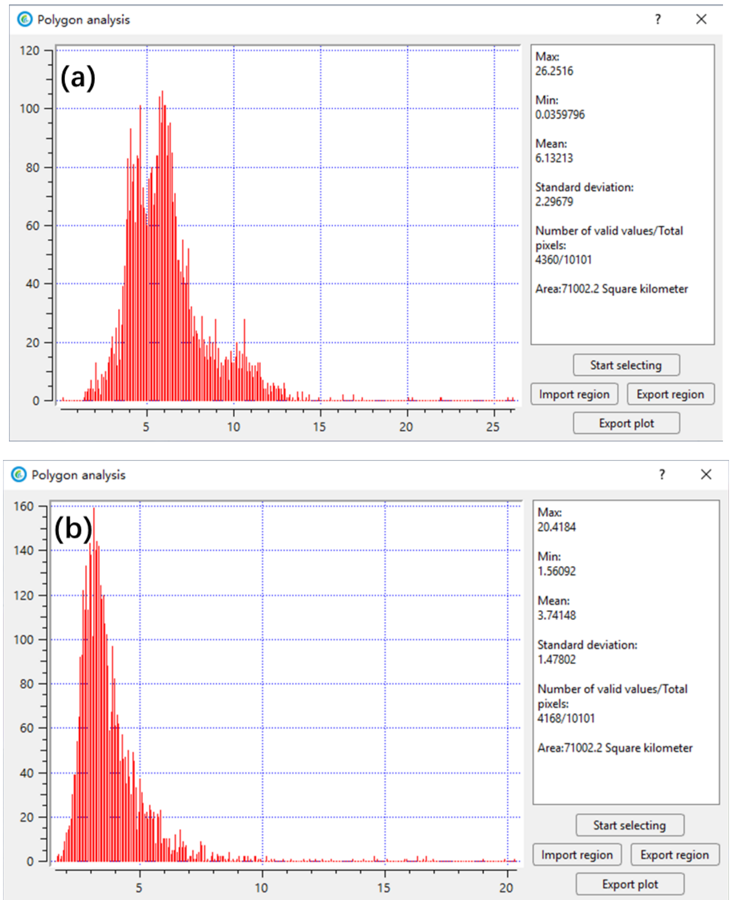

Figure 2-35. Polygon results. Results show that the average chlorophyll concentration in the Bohai Sea was 6.132 mg/m^3 in February 2012 (a) and was 3.741 mg/m^3 in August 2012 (b). According to the histogram and mean value, the chlorophyll concentration in the Bohai Sea was higher in winter than in summer, but the distribution of chlorophyll concentration was more uniform in summer than in winter.

2.4.5 Time series analysis

Time series analysis includes two modules: “time series data” and “animation.”

2.4.5.1 Time series data

It includes points, lines, and polygons time series button.

First, it needs to query the data from the database for time series analysis, including the time range, products, etc. If the “load selected image” is checked at the same time, the data queried will be loaded into the 3D geosphere in the form of layers.

Point time series analysis: Use “mouse click” to select a point on the image or directly input the longitude and latitude of a point, and then click “import” (as shown in Figure 2-36). It will output the sequence value of the sampling point in the selected time period successively, and draw the time series diagram (as shown in Figure 2-37).

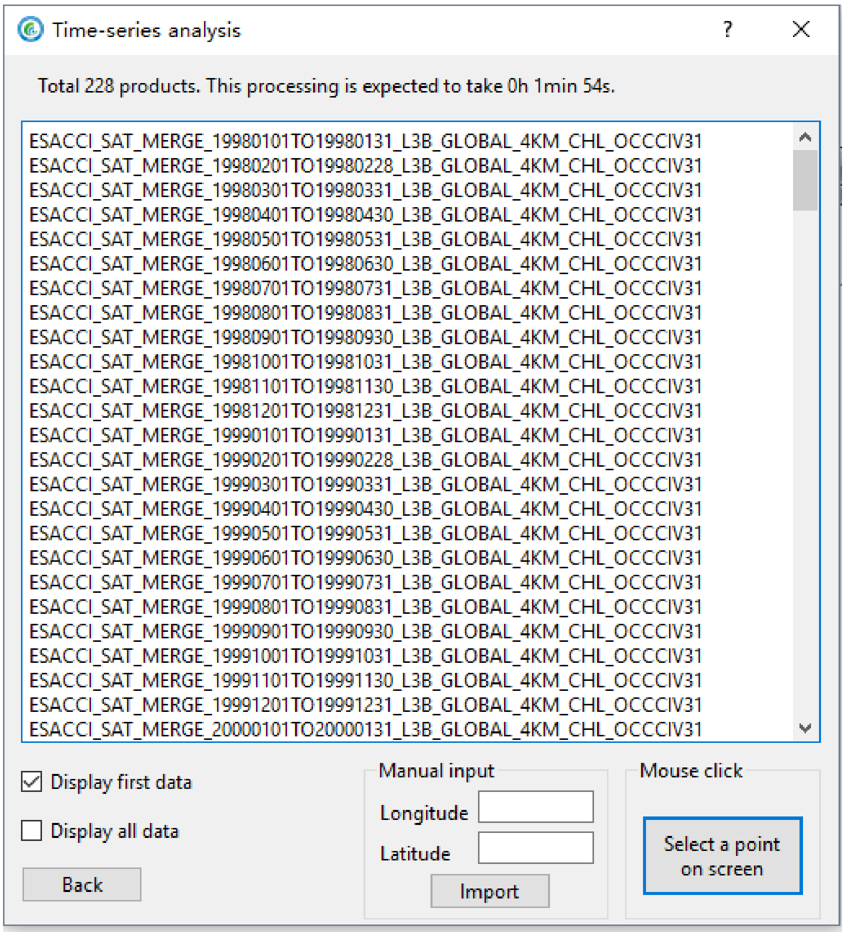

Figure 2-36. Time series query results

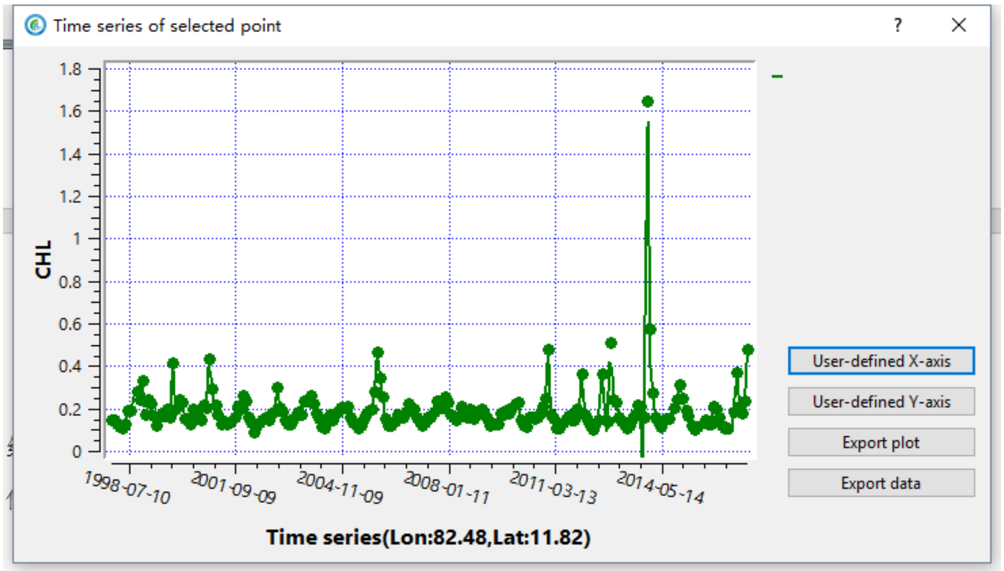

Figure 2-37. Results of temporal variation of selected point

Line time series analysis: Click “draw line(s) on screen,” and mouse click on the image several times and double-click to end; then, the system returns a line sequence diagram (Figure 2-38). The user can also click the “import” button to import the .txt file containing the longitude and latitude coordinates of the point, and corresponding values along the selected line (the format is shown in Figure 2-39). The plots can show wither spatial average, or temporal average, along a selected line.

1) Spatial average along a selected line. The x-axis is the sequence number of each grid point on the polygonal line relative to the starting point, and the y-axis is the time average results in the statistical sequence (as shown in Figure 2-40).

2) Temporal average along a selected line. The x-axis is the time series, and the y-axis is the average value of all grid points on the polygonal line (Figure 2- 41).

The statistical mean, range and standard deviation can be set to display or not.

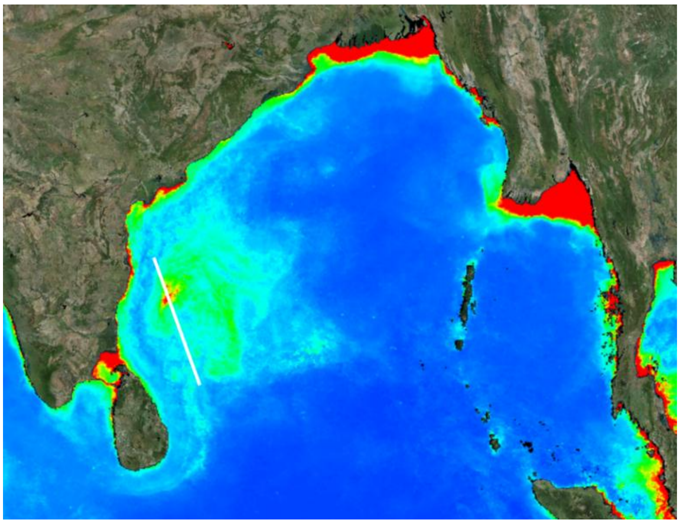

Figure 2-38. The monthly average chlorophyll concentration in the Bay of Bengal in December 2005 obtained from the ESACCI data set with 4-km resolution. The white line represents the polygonal line for line time series analysis, which passes through the algal bloom area.

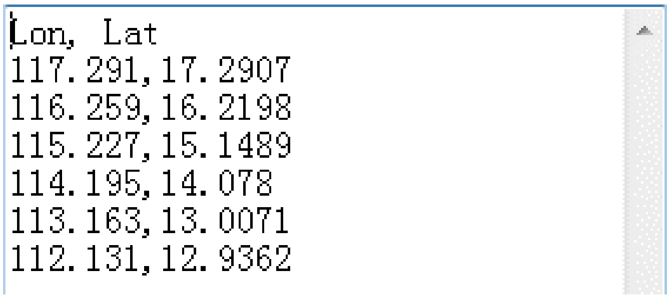

```
Lon, Lat
117.291,17.2907
116.259,16.2198
115.227,15.1489
114.195,14.078
113.163,13.0071
112.131,12.9362
```

Figure 2-39. File format for import

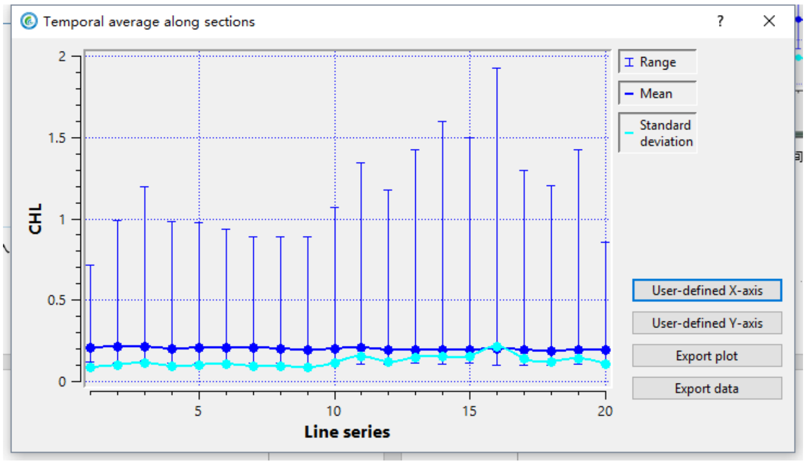

Figure 2-40. Diagram for temporal average along a section. The x-axis represents sequence numbers of grid points relative to the starting point, and the y-axis is the chlorophyll concentration. Dark blue dot represents time average chlorophyll concentration of each grid point on the line within the sequence, and light blue dot represents standard deviation of chlorophyll concentration of each grid point on the line within the sequence. The vertical line represents the range of each grid point value in time sequence.

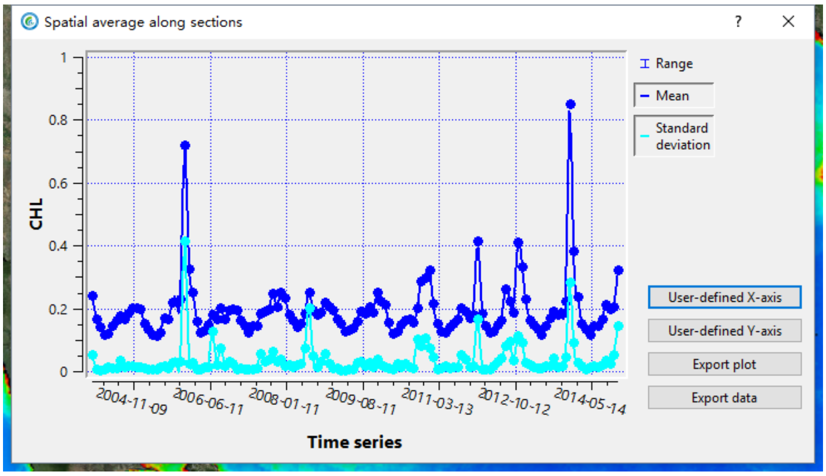

Figure 2-41. Diagram of spatial average along a section. The x-axis represents time, and the y-axis represents chlorophyll concentration. The dark blue dots represent the average chlorophyll concentrations of all grid points on the polygonal line, and the light blue dots represent the standard deviation of average chlorophyll concentration of all grid points on the polygonal line. According to the results, the high chlorophyll value appeared in the southwest of the bay around December every year, and the chlorophyll concentrations in December 2005 and December 2013 were 3-4 times of that in normal years. After Chen et al. (2013). [Episodic phytoplankton bloom events in the Bay of Bengal triggered by multiple forcings. Deep Sea Research Part I, 73(3), 17-30.]

Polygon time series analysis: Click the "polygon" button, and click the image and double-click the end to dray a polygon (Figure 2-42), or click on the "import" button to import the .txt file containing the latitude and longitude coordinates of the polygon points (as shown in Figure 2-39). The software will, in turn, output the selected time series data of the user-defined polygon area, and the basic statistical information of the grid points contained in the polygon region will be plotted as time series (Figure 2-43). The statistical mean, range and standard deviation can be set to display or not.

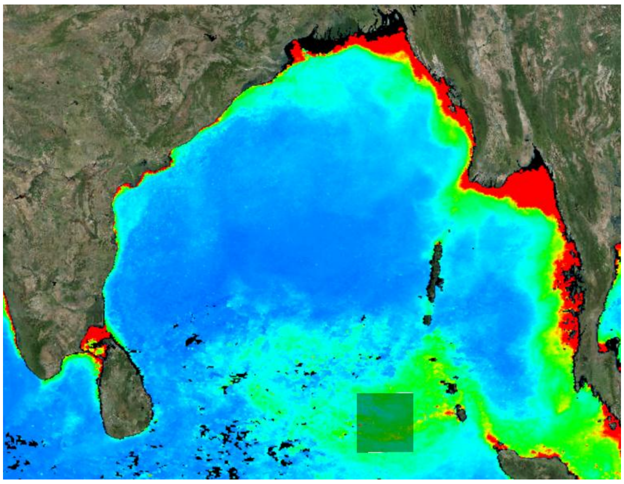

Figure 2-42. The monthly average chlorophyll concentration (4-km resolution) of the Bay of Bengal in January 1998 obtained from the ESACCI data set. The transparent green rectangle represents the area selected for the time series analysis where algal bloom occurred.

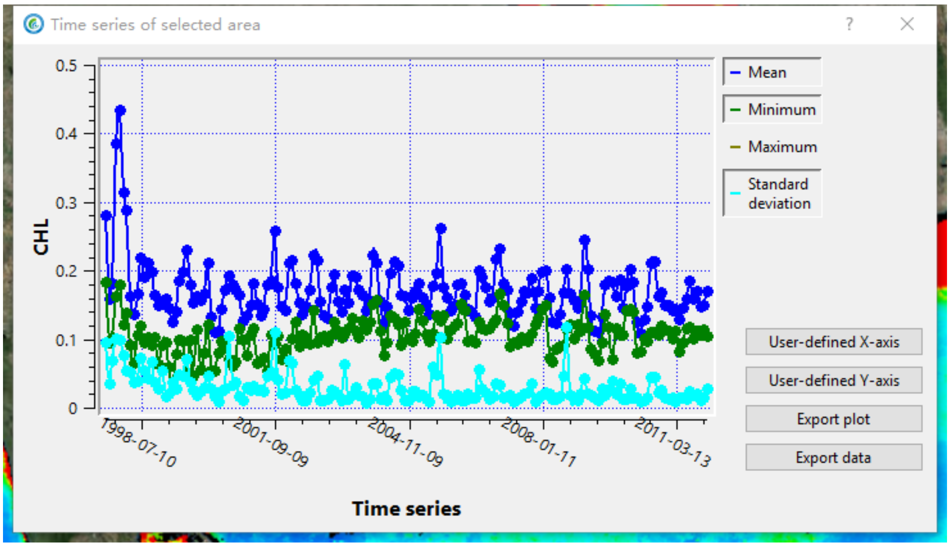

Figure 2-43. Time series of selected area. The x-axis is time, and the y-axis is chlorophyll concentration. The dark blue dots are the monthly average chlorophyll concentration of the effective grid points in the rectangular area, the green dots are the minimum values of the grid points in the rectangular area, and the light blue dots are the standard deviation. The average chlorophyll concentration in the southeast of the Bay of Bengal in January 1998 was 2-3 times that of normal years.

For the above time series result plot, users can click the X/Y axis to adjust the minimum value, maximum value, primary number, and secondary number of coordinate axis to redraw the plot (Figure 2-44). The results can be saved to the local directory in image and text format through the “export plot” or “export data” buttons.

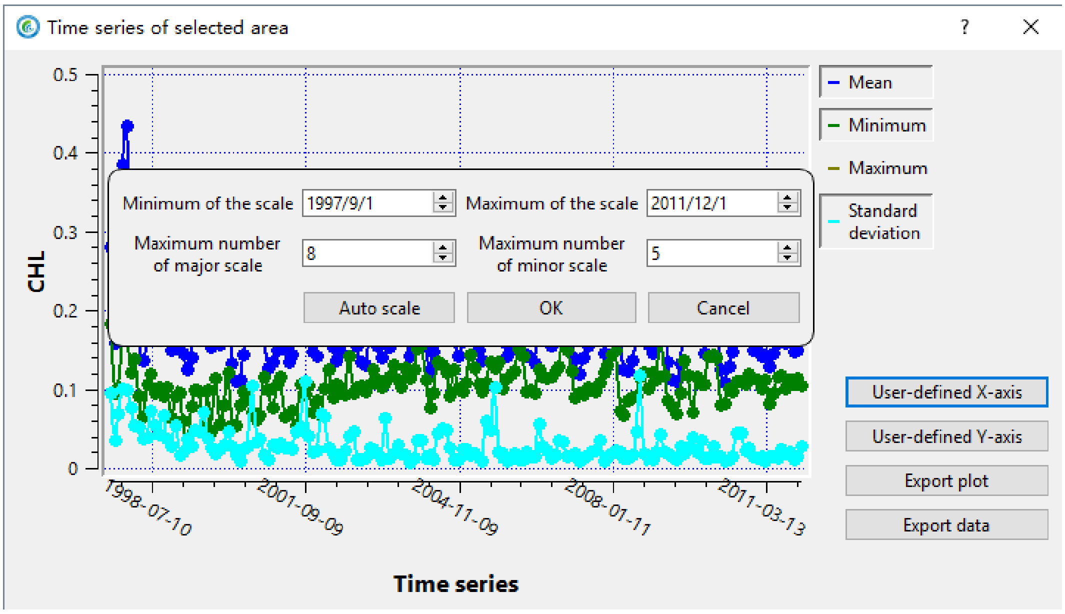

Figure 2-44. Adjust X/Y axis

2.4.5.2 Animation

After clicking the "image animation" button, the image animation dialog box will pop up, and the product query results will appear (as shown in Figure 2-45).

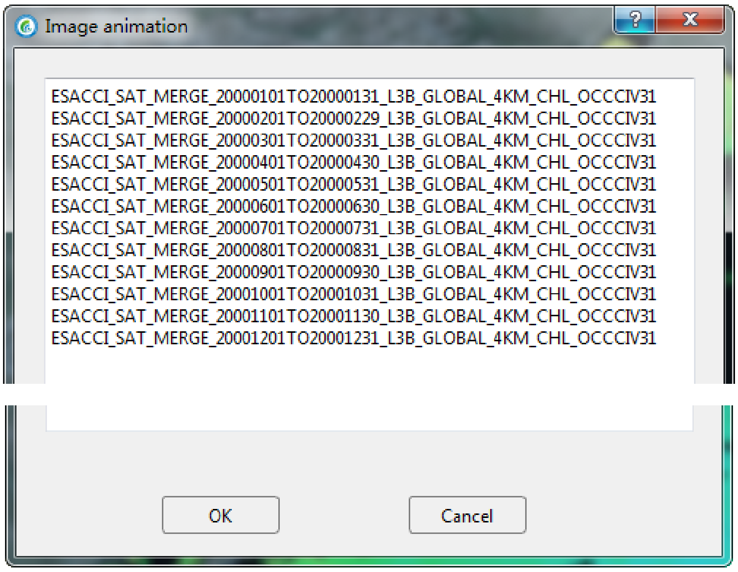

Figure 2-45. Query results dialog

Click the "OK" button, and the products queried will be loaded into the 3D geosphere in the form of layers. After all products are loaded successfully, the animation play panel will pop up. During playback, click the pause (or stop) button to pause (or stop) the current animation. An animation is shown in Figure 2-46.

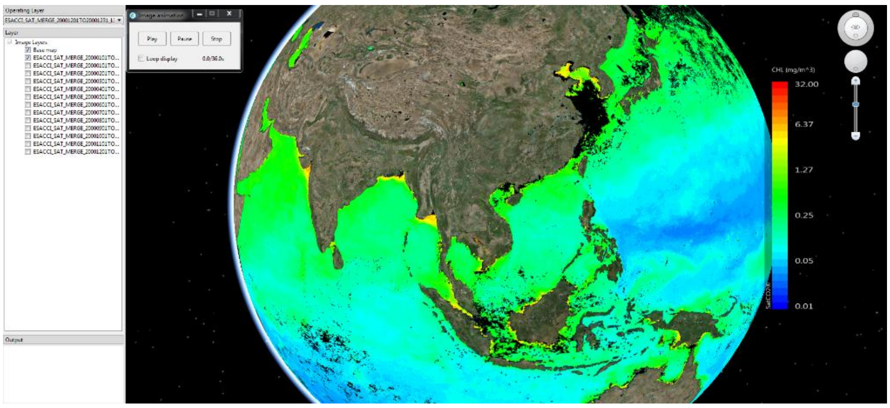

Figure 2-46. Product time continuous animation

Wind field dynamic simulation: Click "vector data" button to pop up the ocean wind field visual dialog box (as shown in Figure 2-47).

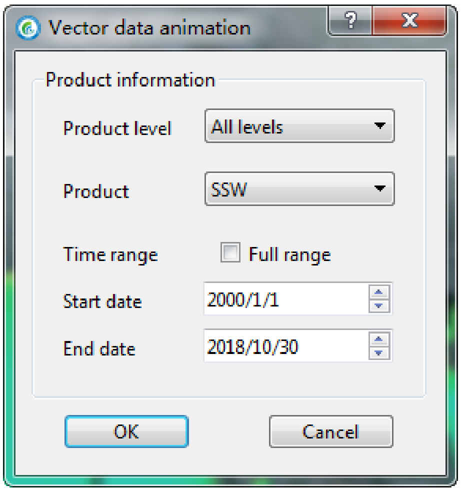

Figure 2-47. Ocean wind field dialog box

Users can select the corresponding conditions, such as “product level,” “product,” and “time range” for product query and selection, and then set animation parameters (Figure 2-48). The result is shown in Figure 2-49.

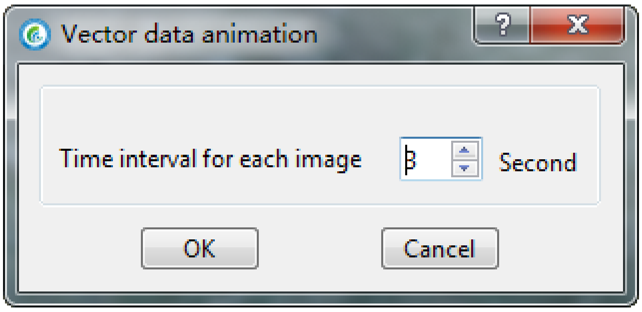

Figure 2-48. Determine animation display speed

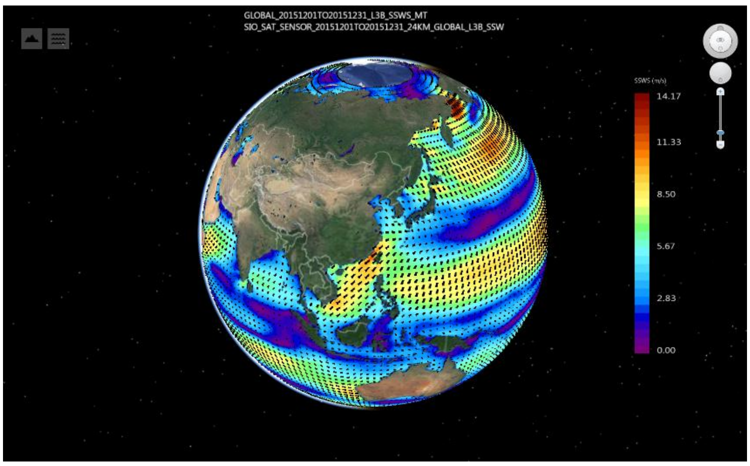

Figure 2-49. Wind animation

2.5 User-defined algorithms

The user-defined algorithm tab includes four modules: “formula editor,” “data gridding,” “data filter,” and “thematic maps” (as shown in Figure 2-50).

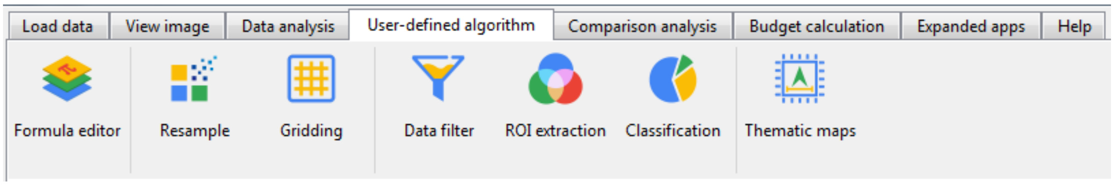

Figure 2-50. User-defined algorithm tab

2.5.1 Formula editor

Click the "formula editor" button, and the calculator dialog will pop up. Click “add local layer,” “add layer,” and “remove” to select satellite data to be used in the calculation. The product parameters correspond to different satellite products, with symbols such as “A, B, C, D “ in the formula (Figure 2-51).

Click the satellite product, operator, and number to combine and build the user-defined calculation expression. After clicking the “calculation” button, you can select the area of your interest for calculation. The calculation result will be loaded into the 3D geosphere in a new grid layer (Figure 2-52). As the satellite data involved in the calculation may have different spatial resolutions, the software acquires the lowest resolution of the data involved in the calculation by default, and users can select the highest resolution for calculation.

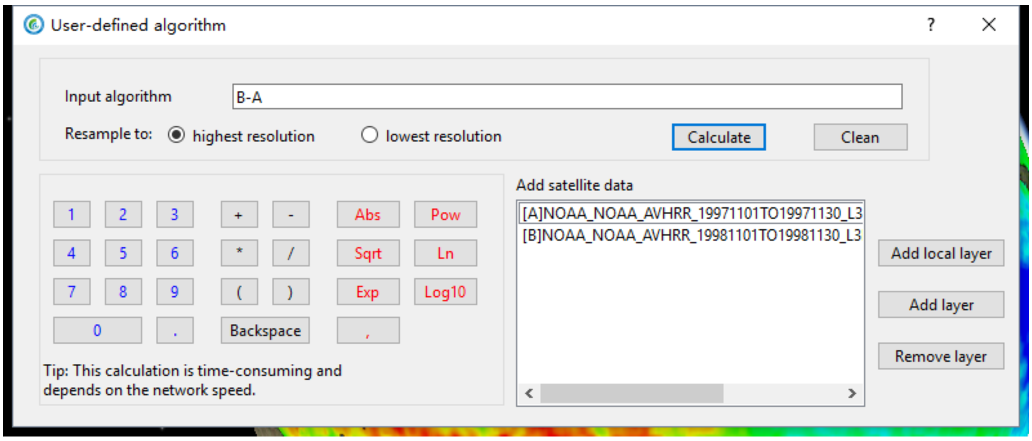

Figure 2-51. Calculation dialog box. Example: A is the monthly average SST data of 25-km resolution of AVHRR in November 1997, and B is the monthly average SST data of 25-km resolution of AVHRR in November 1998. The global mean SST difference in November was calculated using “B minus A.”

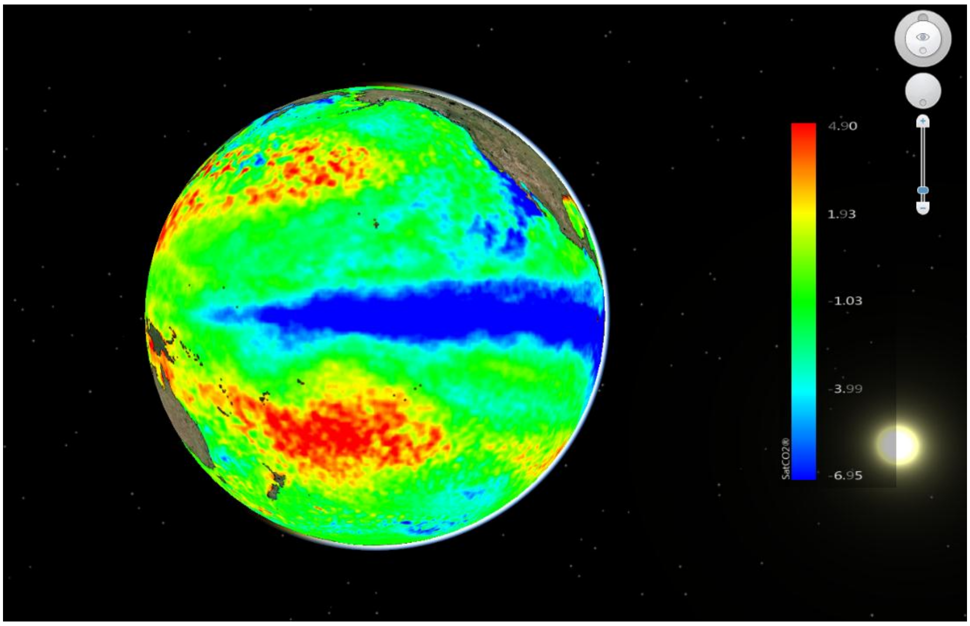

Figure 2-52. Mean SST difference image for the Pacific region between November 1998 (La Nina year) and November 1997 (El Nino year). It shows that the equatorial Pacific Ocean in November 1998 was 7˚C lower than that in November 1997; the Northwest Pacific and Southwest Pacific were 5˚C higher. The SST in the eastern equatorial Pacific changed significantly from El Nino year to La Nina year.

2.5.2 Data gridding

Data gridding includes two modules: "resampling" and "gridding."

Resampling: Modify the spatial resolution of the whole image. After clicking the button, the calculation dialog box (Figure 2-53) pops up. Select the loaded satellite data and click "OK" to start data resampling after setting a new grid resolution. The new resampled image will be automatically displayed on the 3D geosphere (Figure 2-54b).

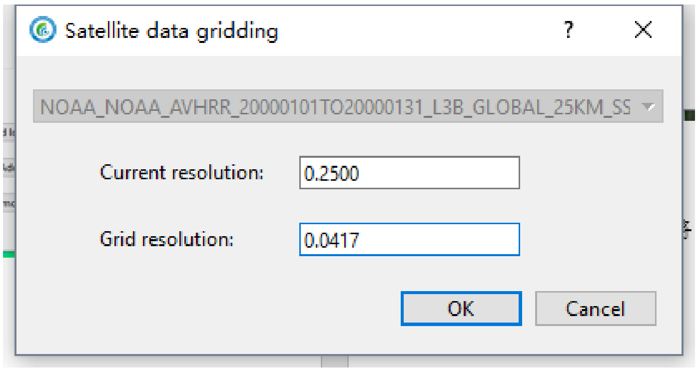

Figure 2-53. Settings for satellite data gridding. The resolution of 0.25 °(25-km) SST data is resampled into 0.0417 °(4-km) resolution.

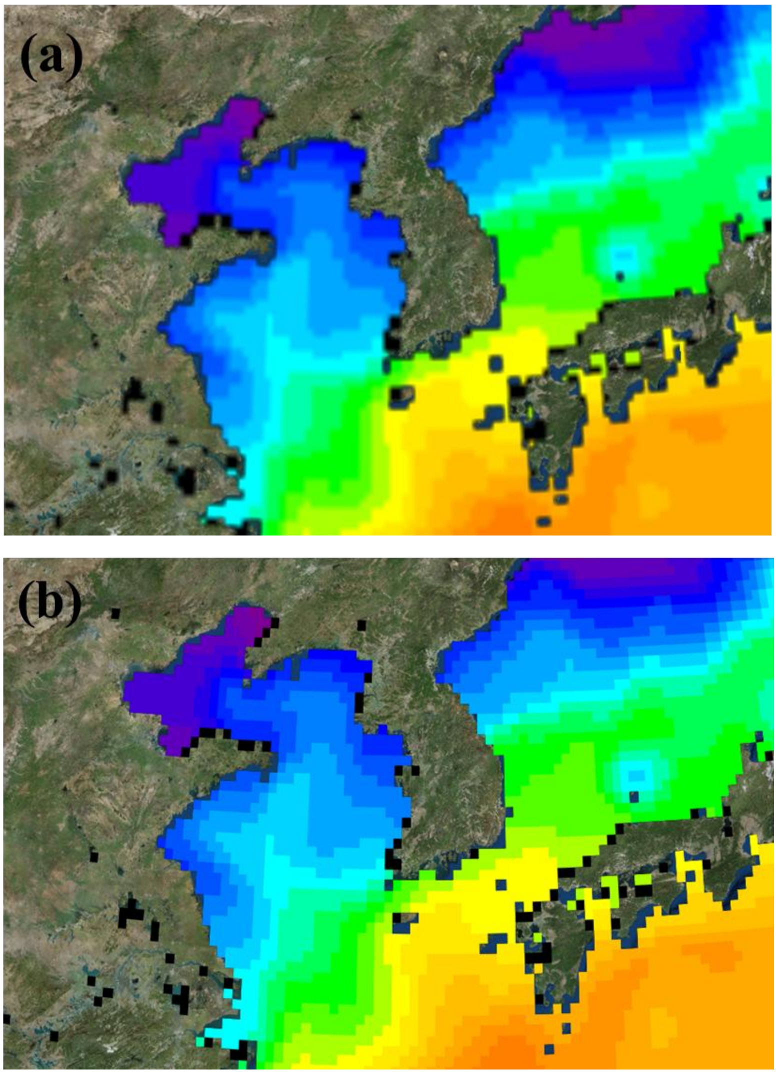

Figure 2-54. Satellite data gridding. (a) AVHRR SST data with 0.25 °(25-km) resolution; (b) SST data after the gridding to 0.0417 °(4-km) resolution. This function can be used to achieve the consistency of spatial resolution of satellite products and facilitate further analysis.

In situ data gridding: Click the “gridding” button, and the calculation dialog box will pop up (Figure 2-55). Select the loaded in situ data, set the required gridding parameters and grid resolution, and click “OK” to grid the data. The system automatically displays the grid results on the 3D geosphere (Figure 2-56). If air-sea CO2 flux (FLX) is gridded, the gridding results can be further evaluated for the carbon budget by area integral.

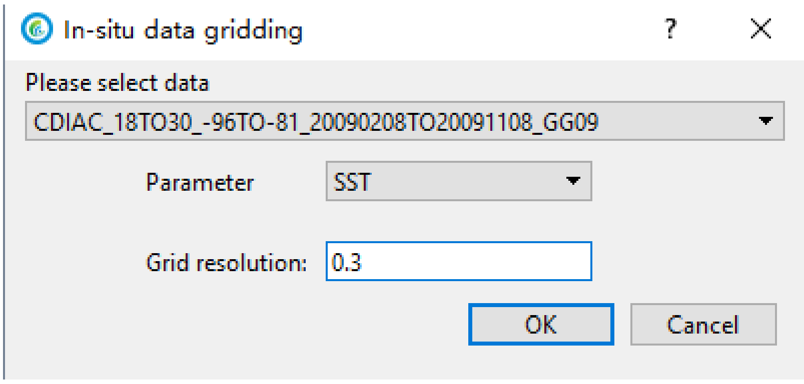

Figure 2-55. In situ data gridding. The in situ SST data of an underway cruise are gridded into 0.3 °resolution grid data

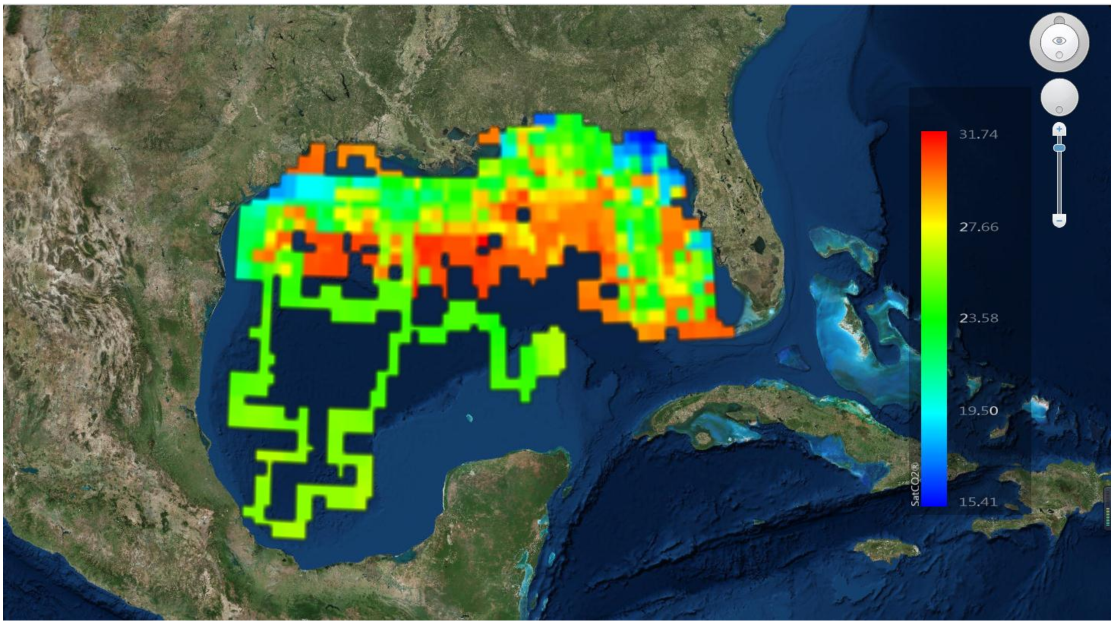

Figure 2-56. In situ data gridding results

2.5.3 Data filter

Data filter includes: "data filter," "ROI extraction," and "classification" modules.

Data filter: Filter the data of the target image according to the custom setting. After clicking the button, the calculation dialog box pops up (Figure 2-57). Select the loaded satellite data and set the logical relationship between the operations, value, and condition (single condition also works) of the filter condition. Click "OK" to start data filtering. Data filtering result automatically displayed on 3D geosphere (Figure 2-58).

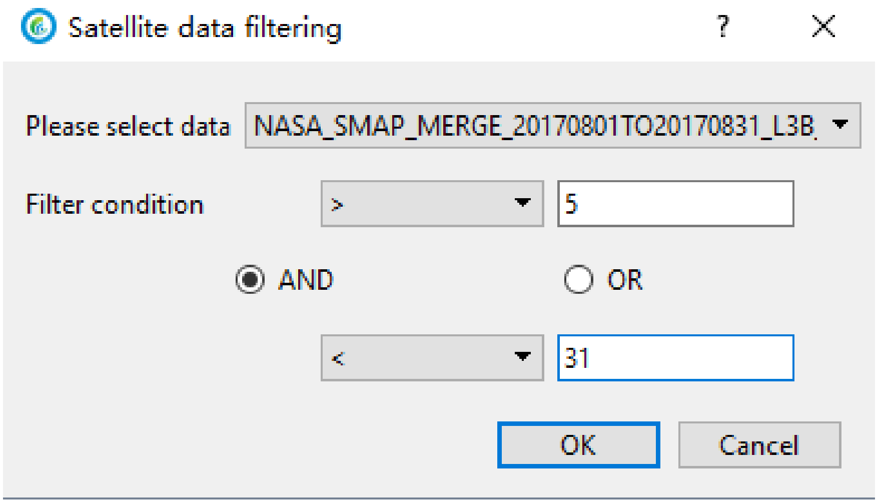

Figure 2-57. Satellite data filtering. The data of the monthly average salinity of the SMAP data set in August 2017, with values greater than 5 and less than 31 being selected.

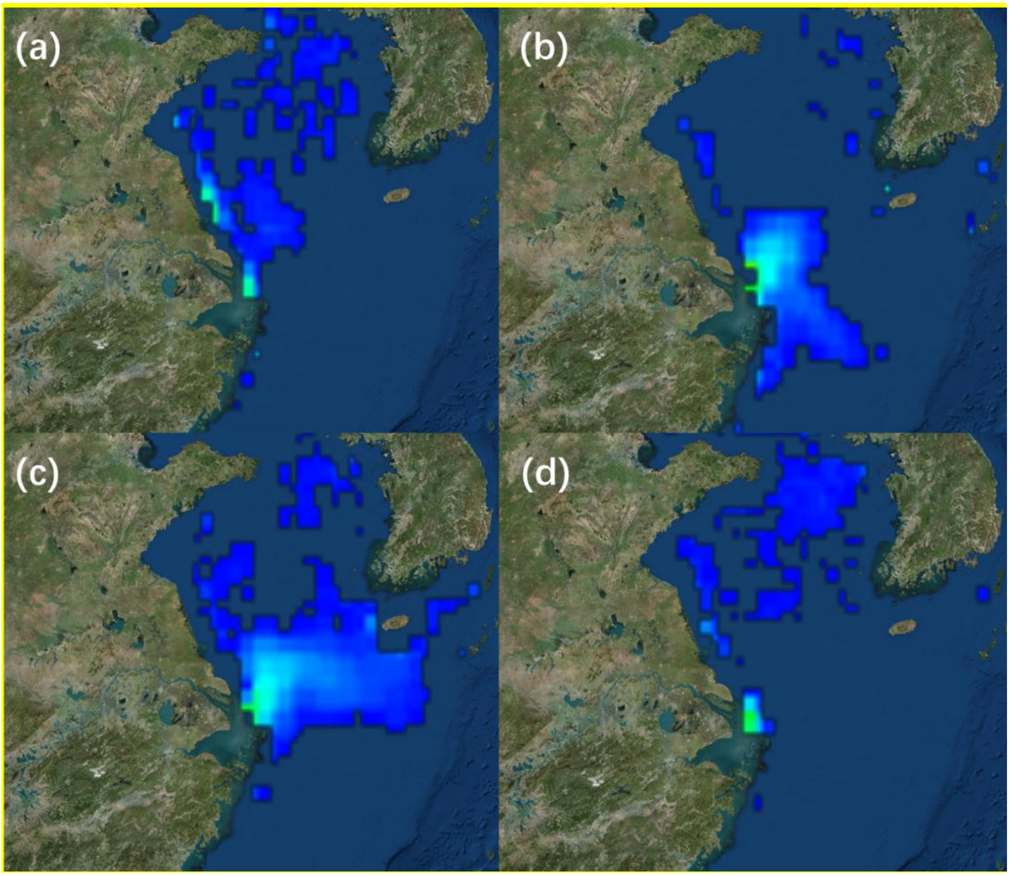

Figure 2-58. Data filtering results: (a) February 2017, (b) May 2017, (c) August 2017, and (d) November 2017. The color scale indicates the areas with salinity greater than 5 and less than or equal to 31. By filtering the salinity data, the Changjiang River plume in different months can be seen clearly.

ROI extraction: Extract the area in the target layer according to the custom setting. Different from the previous function, the extracted region is only a single value image.

Users can restrict conditions for the target layer of single image, or select interest areas for different images and conditions. After clicking the button, the calculation dialog box pops up (Figure 2-59). On the right, [+] or [-] can increase or decrease the number of conditions, respectively. Select the loaded satellite data, set the logical relationship between the symbols, values, and conditions of the selection, and then click “OK” to extract the region of interest. It automatically displays the extracted result on the 3D geosphere (Figure 2-60).

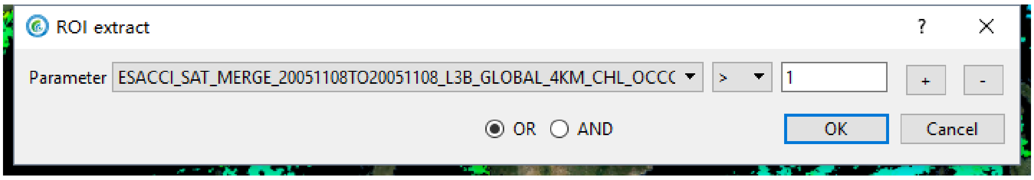

Figure 2-59. ROI extract. The chlorophyll concentration above 1 mg/m^3 on November 8, 2005 in the study area is extracted from the ESACCI data set.

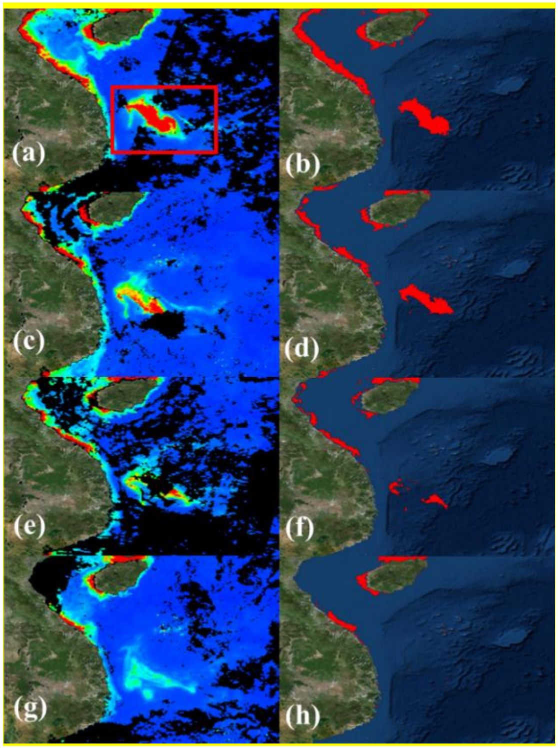

Figure 2-60. Images of (a) November 8, 2015; (c) November 9, 2015; (e) November 10, 2015 and (g) November 12, 2015, showing the 4-km resolution chlorophyll concentration in the western South China Sea from the ESACCI data set. ROI extraction results of (b) November 8, 2015; (d) November 9, 2015; (f) November 10, 2015; and (h) November 12, 2015, showing the area where the algal bloom occurred. The red color represents the area where chlorophyll concentration is greater than 1mg/m^3. The evolution of algal blooms from explosion to extinction can be observed by the extraction of interest area, and the area of algal blooms can be calculated by counting the areas of ROI extraction results.

Classification: the classification of satellite data is mainly based on a customized classification standard for one or more images. After clicking on the button, dialog box pops up (Figure 2-61). [+] [-] on the right side can increase or decrease in number of classification criteria. Choose the loaded satellite data, in turn, fill in the interval value, set up the standard logic relationship, and click on “OK” to start data classification. It will automatically show results on the 3D geosphere (Figure 2-62).

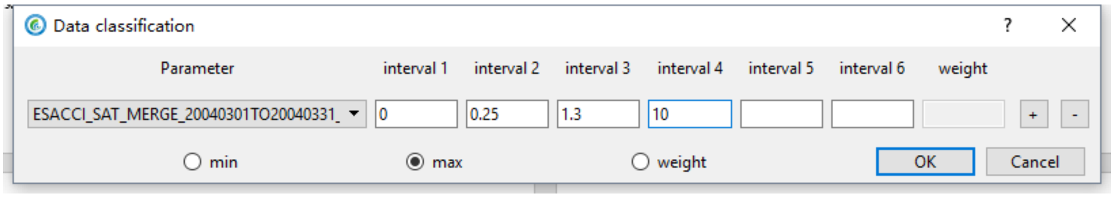

Figure 2-61. Data classification setting. In Hirata et al. (2008), chlorophyll concentration data were used to distinguish the dominant phytoplankton species: chlorophyll concentration ranging 0-0.25mg /m^3 is dominated by pico-phytoplankton (0.2-2 μ m); chlorophyll concentration ranging 0.25-1.3mg /m^3 is dominated by nano-phytoplankton (2-20 μ m); chlorophyll concentration greater than 1.3 mg/m^3 is dominated by micro-phytoplankton (50-1000 μ m). After Hirata et al (2008). [An absorption model to determine phytoplankton size classes from satellite ocean colour. Satellite of Environment, 112(2008), 3153-3159]

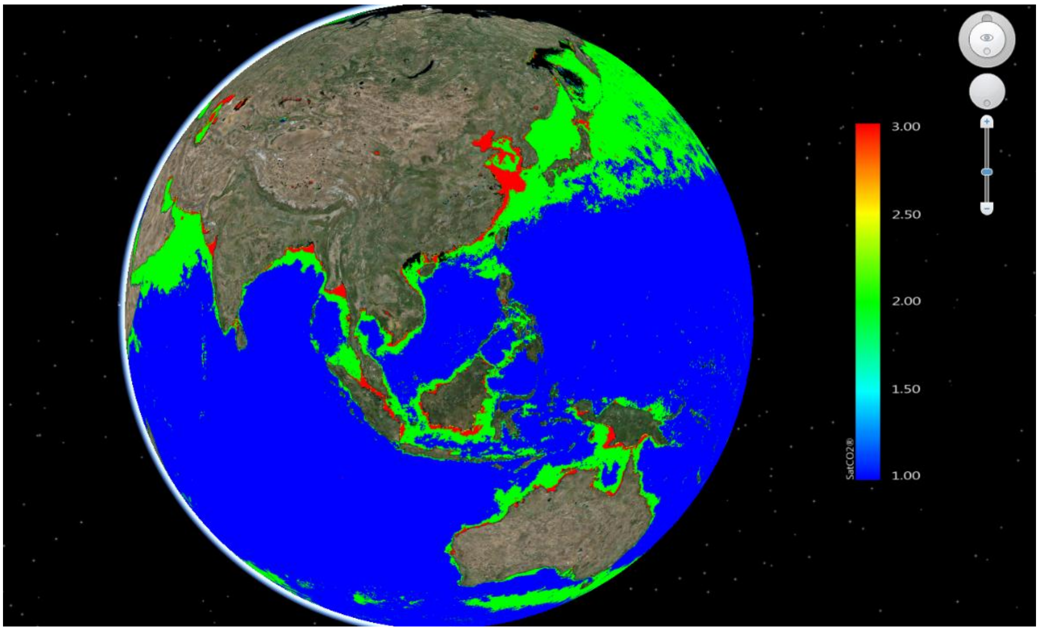

Figure 2-62. Classification results of major phytoplankton categories in March 2004. The original data are from monthly average chlorophyll concentration data of 4-km resolution from ESACCI. The red color represents micro-phytoplankton dominant area, the green color represents the nano-phytoplankton dominant area, and the blue color is for pico-phytoplankton dominant area.

2.5.4 Thematic maps

Click the "thematic maps" button to pop up the satellite product query box. Select a single product to enter the thematic diagram setting dialog box (Figure 2-63).

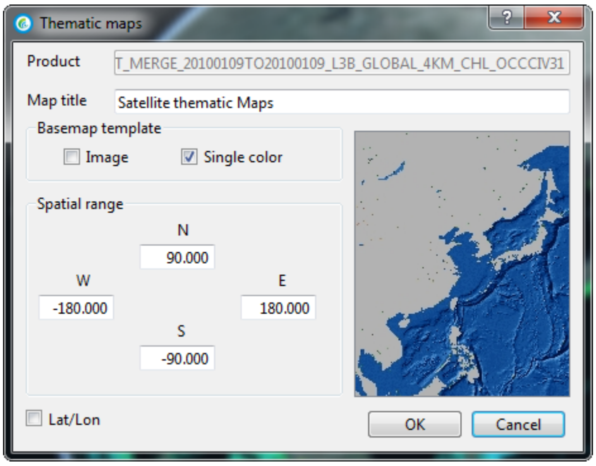

Figure 2-63. Thematic maps setting.

Users can design thematic map elements, such as map title, basemap template, spatial range, and lat/lon grid line. Click the "OK" button to enter the thematic preview view. Click "export" and select saving path (folder) to save the thematic map. An exported thematic diagram is shown in Figure 2-64. This function only works for the data from the online data set, not for the local data.

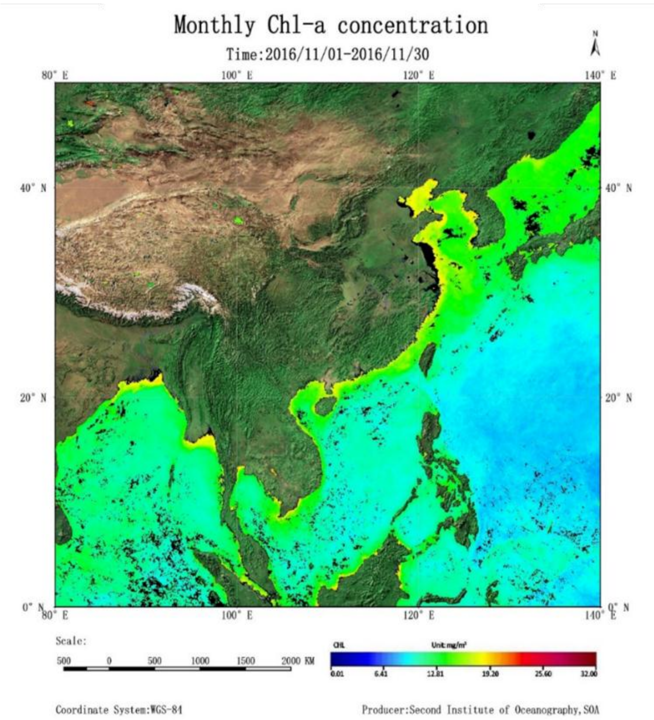

Figure 2-64. The output thematic map of monthly average chlorophyll concentration in November 2016 from the ESACCI data set.

2.6 Comparison Analysis

There are two modules: satellite/in situ data comparison, and satellite/satellite data comparison (as shown in Figure 2-65).

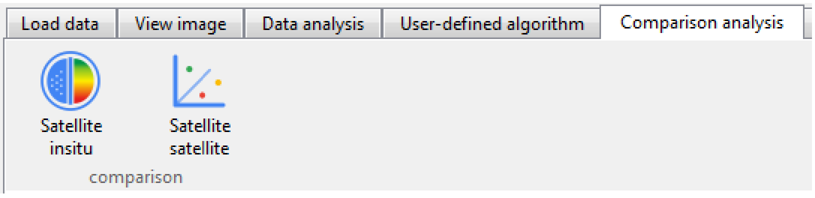

Figure 2-65. Comparison analysis tabs.

2.6.1 Satellite and in-situ data comparison

This function carries out satellite data matching and comparative analysis for the in situ data that have been loaded into the layer list (see section 2.3).

Click the button "satellite/in situ," and the data matching dialog box will pop up (Figure 2-66). First, the system loads the in situ data set (the system will automatically read the start and end times of the in situ data), and then the selected satellite data to be matched. 1) The loaded satellite image can be directly selected for matching the same longitude and latitude (time matching is not considered). 2) Select the setting such as data set, parameter, product level, composite period, and spatial window to be matched. Output are the scattering diagram of in situ and satellite matched data (Figure 2-67).

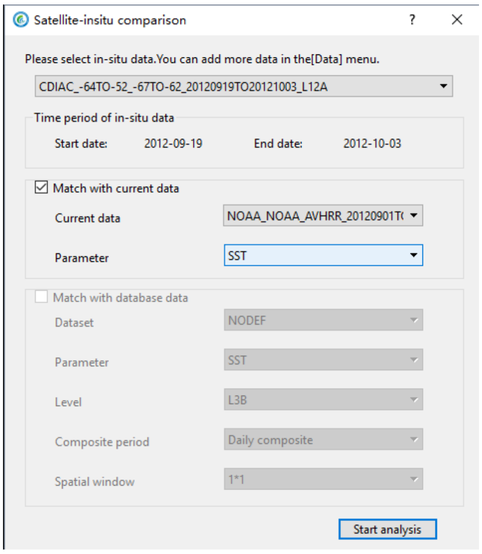

Figure 2-66. Data matching box for "satellite to in-situ comparison." In this case, the temperature data of the CDIAC data set from September 19, 2012 to October 3, 2012 were selected for comparison with the monthly average SST data of NOAA (25-km resolution) in September 2012.

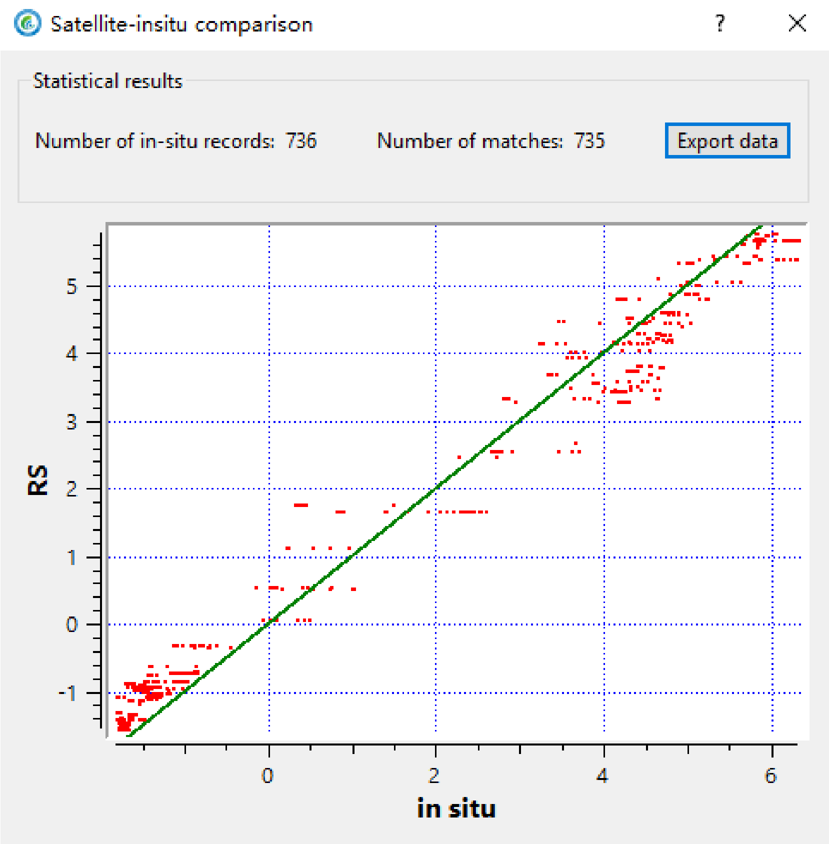

Figure 2-67. Scatter diagram comparing the matched points of satellite (RS) and in situ data. The x-axis represents the in situ temperature data, and the y-axis represents the satellite SST data. The green line represents the 1:1 line. There are 736 in situ data points and 735 matched satellite points obtained.

2.6.2 Satellite vs satellite data comparison

Click “Satellite/satellite” button, the dialog box will pop up. Users can compare the overlapping areas of the two selected satellite data sets to generate a scatter diagram.

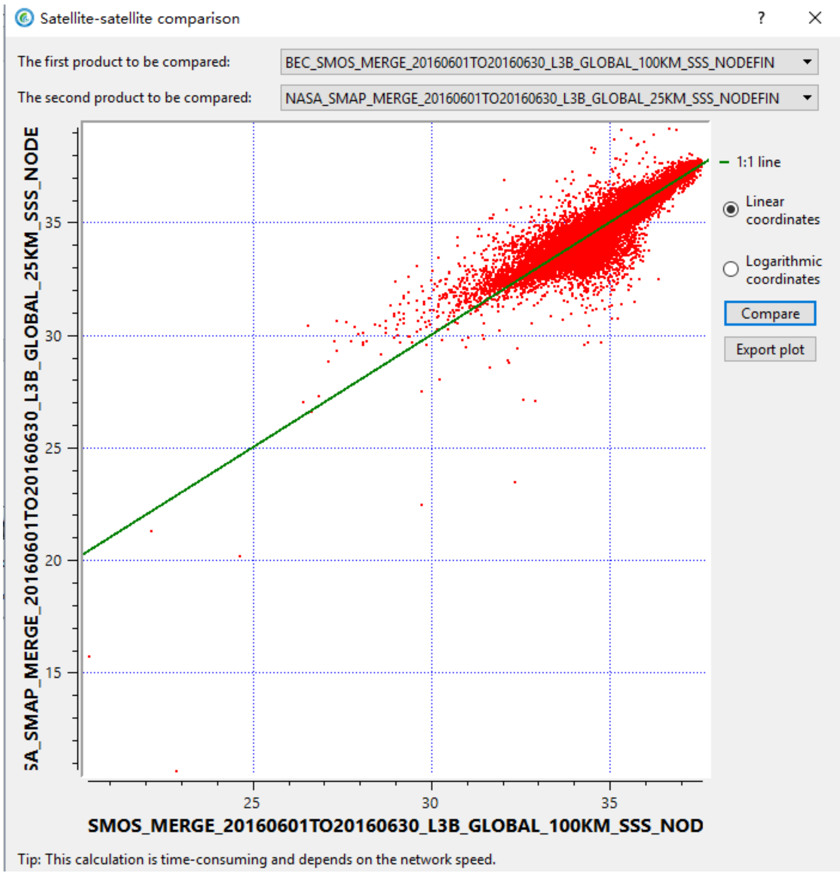

Figure 2-68. Scatter plot of satellite products. The x-axis is the monthly average global salinity products of SMOS satellite (100-km resolution) in June 2016; the y-axis is the monthly average global salinity products of SMAP data set data (25 km) in June 2016. The green line is the 1:1 line. These two types of satellite salinity products show good consistency.

2.7 Budget calculation

The budget calculation includes two modules: air-sea CO2 flux, and carbon budget for the area integral of flux products (Figure 2-69).

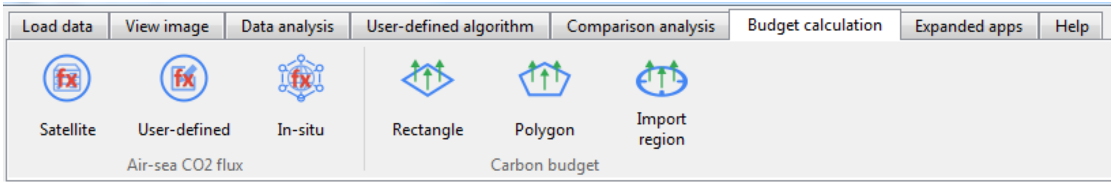

Figure 2-69. Budget calculation tabs.

2.7.1 Air-sea CO2 flux

Air-sea CO2 includes three sub-modules: “Air-sea CO2 based on satellite data,” “Air-sea CO2 based on user-defined data,” and “Air-sea CO2 based on in-situ data.”

Air-sea CO2 flux of satellite data calculation: click the button, and dialog box will pop up (Figure 2-70). Choose interested time period for the query. The database can automatically search the database for related satellite parameters (sea surface temperature, salinity, sea surface wind speed, atmospheric partial pressure of CO2, and the sea partial pressure of CO2).

If the database lacks satellite data of a certain parameter, it cannot carry out follow-up flux calculation. If there are multiple satellite products in the database for the same parameter, you can select one product in the drop-down menu for calculation. Then, set the calculation formula of gas transfer velocity to determine whether C2 wind speed correction is required, and click “OK” to start calculating flux.

By default, the software resamples various spatial resolutions to the highest resolution of the selected data. Users can choose to resample to any resolution for their calculation. Results automatically displayed on 3D geosphere, as shown in Figure 2-71.

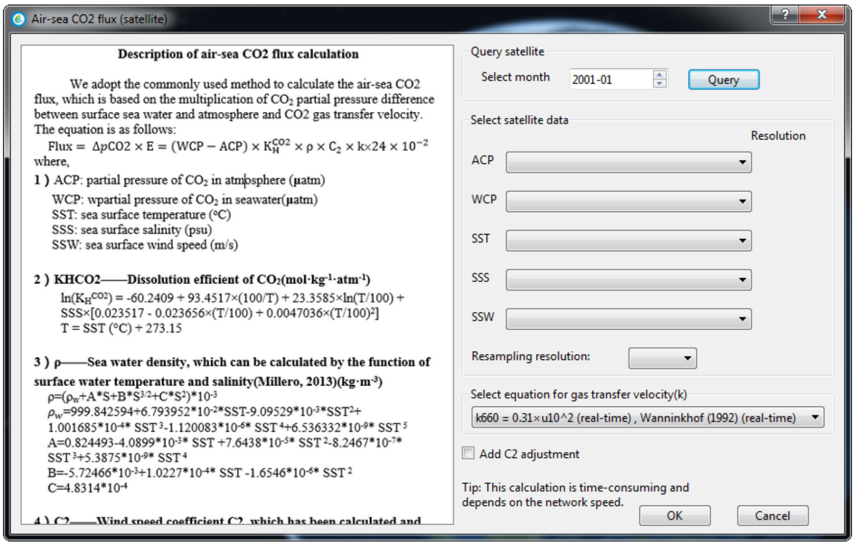

Figure 2-70. Air-sea CO2 flux calculation from satellite data.

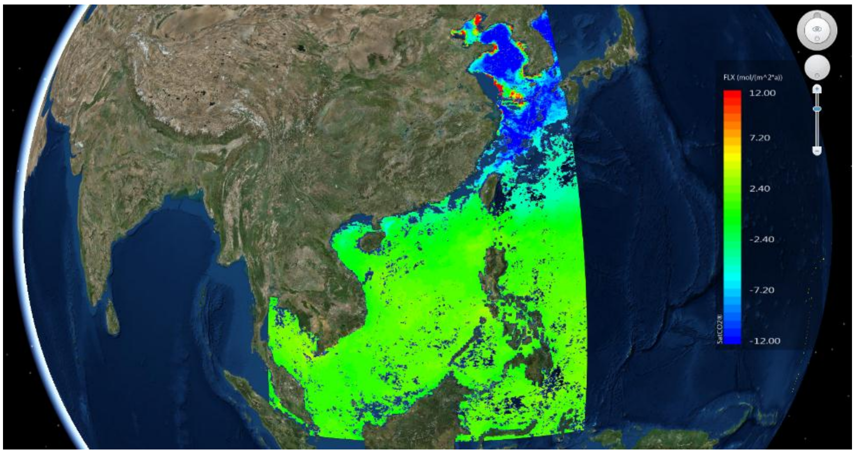

Figure 2-71. Air-sea CO2 flux calculating results.

User-defined calculation: different from the previous module, this module can customize input parameters (sea surface temperature, salinity, sea surface wind speed, atmospheric partial pressure of CO2, and the sea partial pressure of CO2). These data need to be imported through the “load data” menu and loaded in the 3D geosphere in advance, and then can be confirmed by the drop-down menu for selection.

Click “Air-sea CO2 based on user-defined data” button, and the calculation dialog box will pop up (Figure 2-72). Select the satellite data corresponding to the flux calculation parameters, which have been loaded. Set the calculation formula of gas transfer velocity and whether C2 wind speed correction is required. Click “OK” to start flux calculation. By default, the software resamples various spatial resolutions to the highest resolution of the calculated data. Users can choose to resample to any resolution for calculation. Calculation results will be automatically displayed on the 3D geosphere.

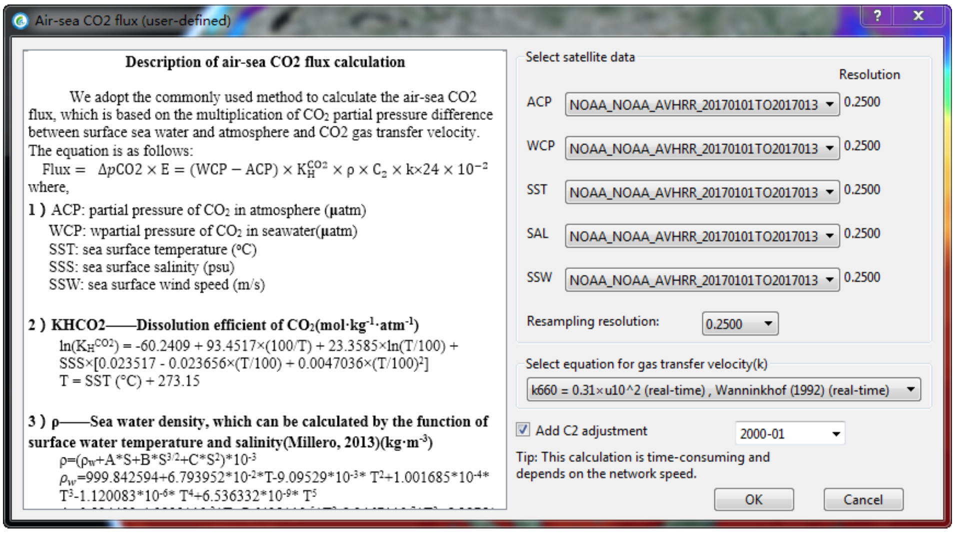

Figure 2-72. Air-sea CO2 flux based on user-defined data.

In-situ data calculation: the flux calculation based on in situ data is similar to the satellite flux calculation. Users load parameters from an online database or local in situ data. If some parameters are missing in the in situ data, the software can provide the temporal-spatial matching satellite data instead (Figure 2-73). For locally loaded in situ data, users need to select the corresponding in situ parameters to match. In addition, users can manually input constant atmospheric partial pressure of CO2 or constant sea surface wind value for the calculation.

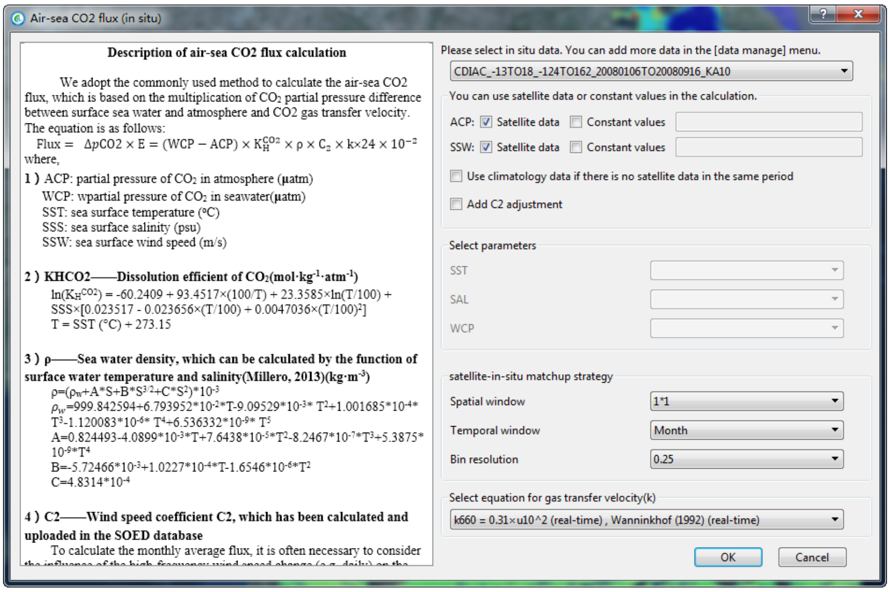

Figure 2-73. Air-sea CO2 flux based on in-situ data.

2.7.2 Carbon budget

The carbon budget module can only be used when air-sea CO2 flux product preloading is completed. The ways to select an area for carbon budget evaluation include rectangle area, polygon area, and import region.

Click the rectangle button to select a rectangle area to be calculated on the 3D geosphere. After double-clicking the rectangle selection, the selected layer is performed to calculate the area integral of air-sea CO2 flux.

Click the polygon button to select the polygon area to be calculated by clicking the left mouse button on the 3D geosphere. After double-click to complete the polygon selection, the selected region would be applied to the area integral air-sea CO2 flux calculation (Figure 2-74).

Import region: after clicking the import region button, select preset sea area. Users can also import the area information file in the pre-drawn .shp format, and area integral calculation is performed for the area covered (Figure 2-75). Note: .shp format files can be produced by ArcGIS and other software.

Click the calculation button to calculate the area integral of CO2 flux for the specified area of the product layer. The result is shown in Figure 2-76.

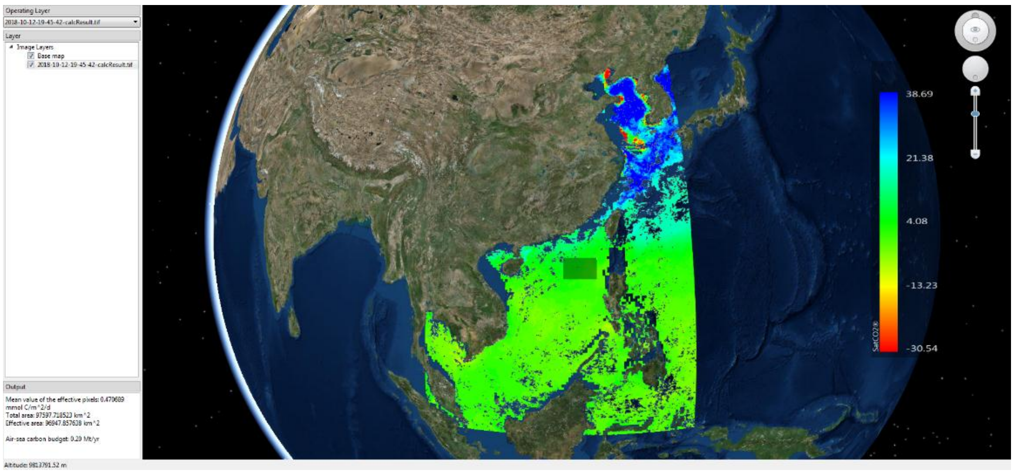

Figure 2-74. Area integral.

Figure 2-75. Select a region.

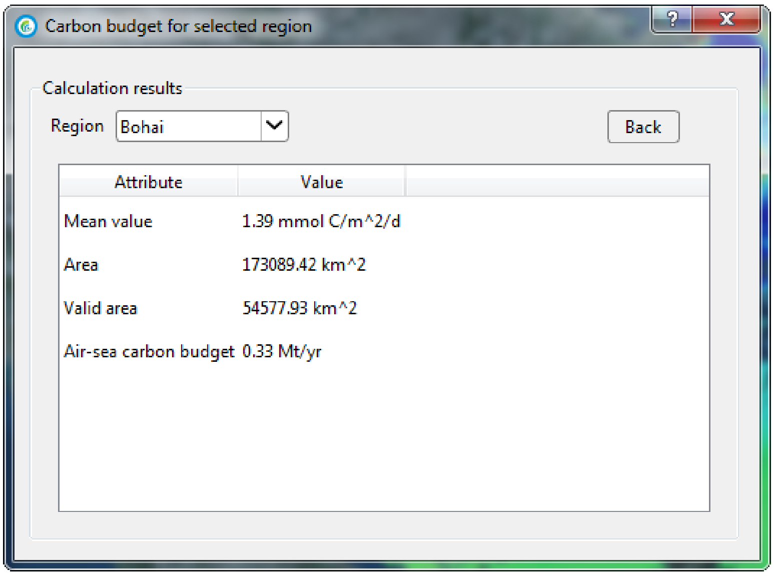

Figure 2-76. Carbon budget calculation for selected region.

2.8 Harmful algal boom detection

Click the HAB (harmful algal boom) detection button. After the window pops up, click the “select data” button to select the data file (.nc format) for HAB detection. After selecting the relevant algorithm (Figure 2-77), click “OK,” and it will automatically load the calculation results of HAB detection onto the 3D geosphere (Figure 2-78).

The system contains a number of published algorithms for HAB detection (see Appendix 7). The user can choose one algorithm by using the drop-down menu.

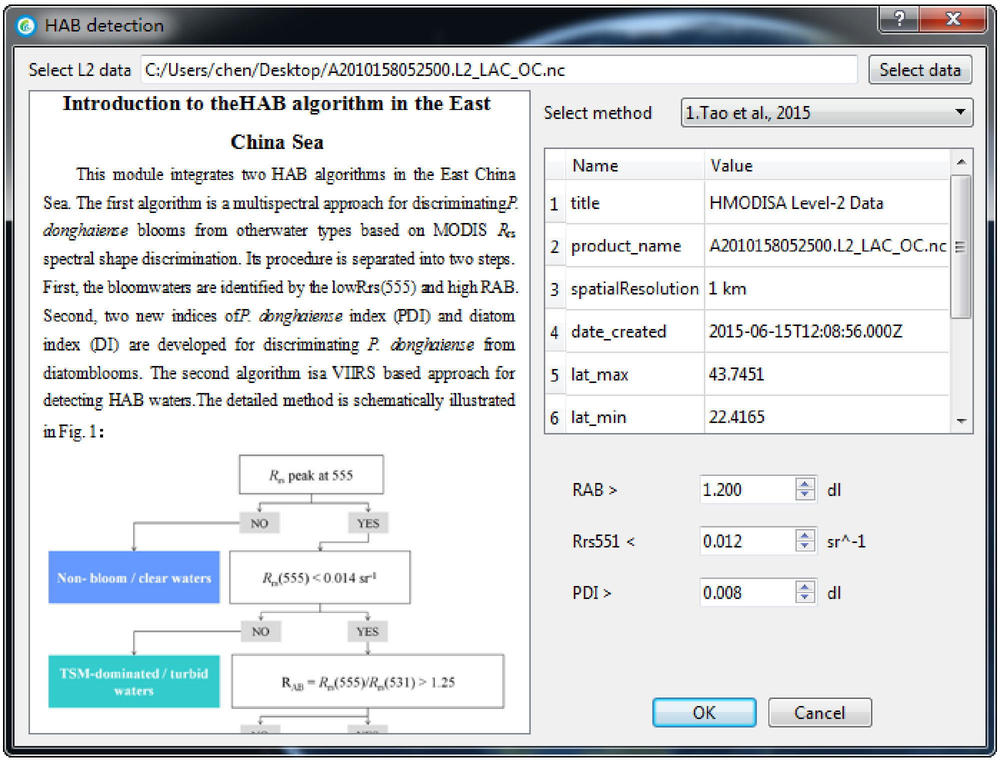

Figure 2-77. HAB detection.

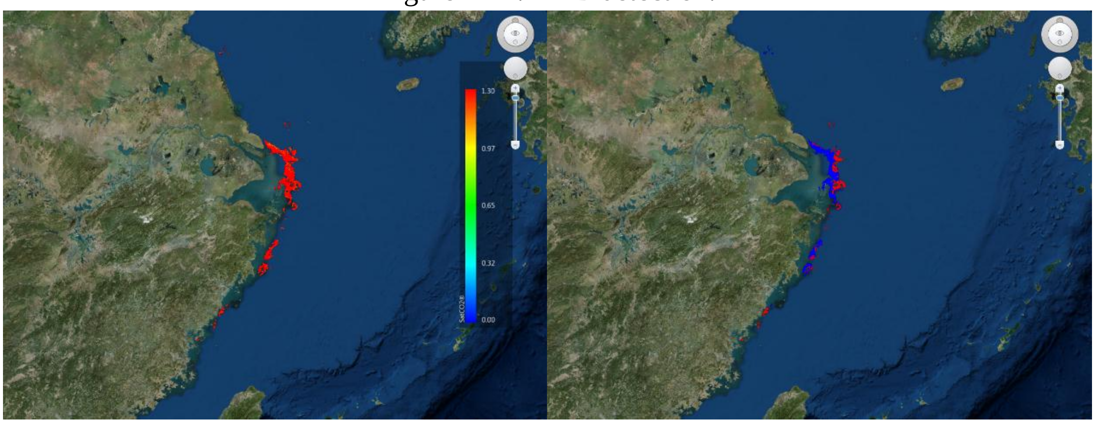

Figure 2-78. Results of HAB detection.

Appendix 1: Source of base map

The base map data come from the public map service of ESRI (Environmental Systems Research Institute, Inc.). When you use the data, you must abide the terms of service (https://www.esri.com/zh-cn/legal/terms/full-master-agreement).

The SIO and ZJU shall not assume all responsibilities arising from the user’s release, copy, or modification of the data in violation of the provisions.

Appendix 2: Data source

SatCO2 platform and data are free of charge. The goal is to promote the sharing and multi-disciplinary application of marine remote sensing data.

The SatCO2 database collects satellite data and products from different agencies, produces them with the algorithms developed by SOED/SIO, then transform and unify data formats, and uploads in SEOD-processed data products for online analysis applications. SatCO2 platform does not provide bulk download for these original data sets. Acknowledgments and citations are required, including the SatCO2 platform, the associated algorithmic signer, and the original data provider, when results produced by users using the SatCO2 platform were published. For more detailed and updated information, please refer to: www.SatCO2.com.

The main sources of original satellite data currently used in the database (November 2018 version) include:

1. National Satellite Ocean Application Service (NSOAS)

Level-1 data of Chinese satellite GaoFen-4 provided by NSOAS.

http://dds.nsoas.org.cn/main.do

2. National Marine Satellite Ground Station (Hangzhou)

Level-1 data of Chinese satellite HY-1B provided by the national marine satellite ground station (Hangzhou), SOED/SIO.

3. Korean Ocean Satellite Center (KOSC)

Level-1B data of geostationary ocean color imager (GOCI) provided by the KOSC.

Data download: http://kosc.kiost.ac.kr/

Data policy: http://kosc.kiost.ac.kr/eng/p60/kosc_p64.html

4. National Aeronautics and Space Administration (NASA)

Level-L3A data from three sensors of SeaWiFS, MODIS/Aqua, and VIIRS, including remote sensing reflectance at various bands, chlorophyll-a concentration, photosynthetically active radiation, sea surface particle organic carbon, sea surface particle inorganic carbon, and sea surface salinity from Aquarius provided by NASA.

Data download: https://oceancolor.gsfc.nasa.gov/，

Data policy: https://science.nasa.gov/earth-science/earth-science-data/data-information-policy/data-rights-related-issues

Acknowledgment: NASA Goddard Space Flight Center, Ocean Ecology Laboratory, Ocean Biology Processing Group; (2018): SeaWiFS, MODIS/Aqua, VIIRS, Ocean Color Data, NASA OB.DAAC. doi: 10.5067/ORBVIEW-2/SEAWIFS_OC.2014.0. Accessed on 2016/02/29.

5. Remote Sensing Systems (RSS)

SST merged from multiple satellite data, reanalysis wind speed data from CCMP, wind speed data from Windsat, and SSS data from SMAP provided by the Remote Sensing Systems.

Data download: ftp://ftp2.remss.com/

Data policy: http://www.remss.com/support/faq/#data-use

Acknowledgment: SMAP salinity data are produced by Remote Sensing Systems and sponsored by the NASA Ocean Salinity Science Team. Data are available at www.remss.com.

WindSat data are produced by the Remote Sensing Systems and sponsored by the NASA Earth Science MEaSUREs DISCOVER Project and the NASA Earth Science Physical Oceanography Program. RSS WindSat data are available at www.remss.com. CCMP Version-2.0 vector wind analyses are produced by the Remote Sensing Systems. Data are available at www.remss.com.

6. Copernicus Marine Environment Monitoring Service (CMEMS)

Global sea level anomaly, mixed layer thickness/depth, and the model results of geostrophic flow provided by CMEMS.

Download: http://marine.copernicus.eu/services-portfolio/access-to-products/

Data policy: http://marine.copernicus.eu/services-portfolio/service-commitments-and-licence/.

7. Oregon State University (OSU)

Global net primary production products based on three algorithms and on SeaWiFS, MODIS/Aqua, and VIIRS data provided by OSU.

Data download: http://www.science.oregonstate.edu/ocean.productivity/

Acknowledgment: Net primary production data are provided by the Oregonstate University site (http://www.science.oregonstate.edu/ocean.productivity/index.php).

8. European Space Agency (ESA)

SSS data from SMOS and merged Chla data provided by ESA.

Data download: https://smos-diss.eo.esa.int/oads/access/

https://www.oceancolour.org/

Data policy:

https://earth.esa.int/pi/esa?type=file&table=aotarget&cmd=image&id=122

http://www.esa-oceancolour-cci.org/?q=webfm_send/684

Acknowledgment: Ocean Colour Climate Change Initiative dataset, Version 3.1, European Space Agency, available online at http://www.esa-oceancolour-cci.org/.

9. National Oceanic and Atmospheric Administration (NOAA)

Dry air CO2 molar number, relative humidity, and SST provided by NOAA.

Data download: https://www.esrl.noaa.gov/gmd/ccgg/carbontrack

https://rda.ucar.edu/datasets/ds083.2/#!access

https://www.ncdc.noaa.gov/oisst/data-access

Data policy: https://www.esrl.noaa.gov/gmd/ccgg/carbontracker/citation.php

https://rda.ucar.edu/#!data-citation.

Acknowledgment: Research Data Archive at the National Center for Atmospheric Research, Computational and Information Systems Laboratory. https://doi.org/10.5065/D6M043C6. Accessed† 09 Nov 2018.

10. Carbon Dioxide Information Analysis Center (CDIAC)

Global underway partial pressure of sea water CO2 (pCO2) provided by CDIAC.

Download: http://cdiac.ess-dive.lbl.gov/ftp/oceans/LDEO_Database/ Version_2015/

Acknowledgment: Takahashi, T., S.C. Sutherland and A. Kozyr. 2016. Global Ocean Surface Water Partial Pressure of CO2 Database: Measurements Performed During 1957-2015 (Version 2015). ORNL/CDIAC-161, NDP-088(V2015). Carbon Dioxide Information Analysis Center, Oak Ridge National Laboratory, U.S. Department of Energy, Oak Ridge, Tennessee, doi: 10.3334/CDIAC/OTG.NDP088(V2015).

Appendix 3: List of data sets

SatCO2 V1.0 platform (Released in November 2018) contains satellite and model data products related to marine ecosystem and carbon cycle in seas around China, the western pacific-Indian ocean region and the global ocean in the past 20 years. According to the characteristics of data processing, it is divided into six categories.

1．Special data sets of the seas around China

The raw data for the data set includes level-1 products of GF-4 and HY-1B satellites provided by the national satellite ocean application service of China, and the remote sensing reflectance products provided by NASA, and atmospheric products provided by NOAA. Based on those parameters mentioned above, SOED has produced the normalized water-leaving radiance and primary water quality parameters, such as seawater transparency, surface water salinity, suspended matter concentration, aquatic pCO2 and so on, by using the self-developed atmospheric correction and water constituent inversion algorithms.

Names Of data sets	Parameters	Spatial range/resolution	Temporal range/resolution
GF-4 data sets	normalized water-leaving radiance (491, 561, 653, 809 nm), suspended particle matter concentration	Single orbit; 50m	November 2017 - present; single orbit
HY-1B data sets	normalized water-leaving radiance (412, 443, 490, 520, 565, 670 nm), surface chlorophyll concentration, surface suspended matter concentration, 865-nm aerosol optical thickness, sea water transparency, sea surface temperature, attenuation coefficient, atmosphere visibility, CDOM absorption coefficient (including the detritus absorption)	Single orbit; 1.6 km	April 2007 - January 2016; single orbit
China sea CO_2 data sets	surface water salinity, aquatic pCO_2	(100 °-130 °E, 0 °-41 °N); 1.6 km	2003-2018; monthly average

2．GOCI data sets

The original data of the data set are from the GOCI L1B, which are geostationary ocean color satellite remote sensing data provided by the Korea Ocean Satellite Center. On this basis, SOED produces normalized water-leaving radiance and surface suspended matter concentration products in the two coastal regions, which are Bohai Sea and Yangtze River Estuary, with high spatial and temporal resolution based on the self-developed atmospheric correction and inversion algorithms.

<table>
<tr><th>Names Of data sets</th><th>Parameters</th><th>Spatial range/resolution</th><th>Temporal range/resolution</th></tr>
<tr><td>Yangtze River Estuary</td><td rowspan="2">normalized water-leaving radiance (412, 443, 490, 555, 660, 680, 745, 865 nm), surface suspended matter concentration</td><td>(119 °-126 °E, 27 °-35 °N); 500 m</td><td rowspan="2">2011 – present; every hour</td></tr>
<tr><td>Bohai Sea</td><td>(117 °-123 °E, 37 °-41 °N); 500 m</td></tr>
</table>

3． Western Pacific-Indian Ocean data sets

Based on the raw data of remote sensing reflectance products provided by NASA, SOED produces surface suspended matter concentration, chlorophyll concentration, and seawater transparency products in the eastern Indian Ocean, western Pacific Ocean, and South China Sea using the self-developed inversion algorithms.

<table>
<tr><th>Names Of data sets</th><th>Parameters</th><th>Spatial range/resolution</th><th>Temporal range/resolution</th></tr>
<tr><td>South China Sea</td><td rowspan="3">surface suspended matter concentration, surface chlorophyll concentration, sea water transparency</td><td>(98°-127°E, 0°-25°N); 1.8 km</td><td rowspan="3">May 2010 – May 2015; daily average, 10-day average, monthly average, yearly average</td></tr>
<tr><td>Western Pacific Ocean</td><td>(121°-160°E, 2°S-46°N); 1.8 km</td></tr>
<tr><td>Eastern Indian Ocean</td><td>(80°-118°E, 10°S-21°N); 1.8 km</td></tr>
<tr><td>One Belt and One Road region</td><td>surface chlorophyll concentration, sea surface temperature, photosynthetic effective radiation, sea water transparency, primary productivity</td><td>(12°W-150°E, 40°S-80°N); 9 km</td><td>2003 – 2014; monthly average</td></tr>
<tr><td rowspan="2">Disastrous wave product</td><td>count of disastrous wave</td><td rowspan="2">(20°-160°W, 60°S-85°N); 9 km</td><td>2006 – 2016; Climatological monthly mean data</td></tr>
<tr><td>significant wave height</td><td>2006 – 2016; daily average</td></tr>
</table>

4. Global data sets

Raw data in these data set are of the remote sensing reflectance, total absorption coefficient, particulate backscattering coefficient retrieved by the SeaWiFS, MODIS/Aqua, and VIIRS from NASA. SOED has produced products such as global sea surface CDOM absorption coefficient, backscattering coefficient, and seawater transparency by using self-developed inversion algorithms.

Names Of data sets	Parameters	Spatial range/resolution	Temporal range/resolution
SeaWiFS	355-nm CDOM absorption coefficient, seawater transparency, non-algal particle absorption coefficient, 660-nm particle attenuation coefficient, 660-nm organic particle attenuation coefficient, and sea surface salinity	Global, 9 km	September 1997-December 2010; daily average, monthly average
MODIS/Aqua			July 2002 – present; daily average, monthly average
VIIRS			January 2012 – present; daily average, monthly average

5. NASA public data sets

These data sets are provided by NASA, including remote sensing reflectance, surface chlorophyll concentration, photosynthetic available radiation, concentrations of organic and inorganic particulate carbon from the SeaWiFS, MODIS/Aqua, and VIIRS sensors, and sea surface salinity from Aquarius sensor.

Names Of data sets	Parameters	Spatial range/resolution	Temporal range/resolution
Aquarius	Sea surface salinity	Global, 100 km	2011-2015; monthly average
SeaWiFS	Remote sensing reflectance (412, 443, 490, 510, 555, 670 nm), surface chlorophyll concentration, photosynthetic available radiation at sea surface, particulate organic carbon and particulate inorganic carbon	Global, 9 km	September 1997 -Nov 2010; daily average, monthly average
MODIS/Aqua	Remote sensing reflectance (412, 443, 488, 531, 547, 555, 645, 667 nm), surface chlorophyll concentration, photosynthetic available radiation at sea surface, particulate organic carbon and particulate inorganic carbon	Global, 9 km	July 2002 – present; daily average, monthly average
VIIRS	Remote sensing reflectance (410, 443, 486, 551, 671 nm), surface chlorophyll concentration, photosynthetic available radiation at sea surface, surface particulate organic carbon and particulate inorganic carbon	Global, 9 km	January 2012 – present; daily average, monthly average

6. Public data sets by other institutions

The raw data of the data sets are from institutions such as RRS, CMEMS, OSU, ESA, NOAA, and ECMWF among others, including ocean environmental parameters, such as sea surface temperature, salinity, sea level, mixing layer depth, wind, rainfall capacity; ecological parameters, such as net primary productivity, multiple-satellite-merged chlorophyll concentration; atmospheric parameters, such as mole fraction of atmospheric CO_2, relative humidity, and sea surface atmospheric pressure.

Names Of data sets	Institution	Parameters	Spatial range/resolution	Temporal range/resolution
CCMP	Remote Sensing Systems (RRS)	sea surface wind	Global, 25 km	1987 - 2017; daily average, monthly average
SMAP		Sea surface salinity		September 2016 - present; monthly average
Sea level anomaly	Copernicus Marine environmental monitoring service (CMEMS)	Sea level anomaly	Global, 25 km	1993 – present; daily average, monthly average
Geostrophic flow		Geostrophic flow		January 1993 – January 2018; daily average, monthly average
Mixing layer depth		Mixing layer depth		1998 – 2015; daily average, monthly average
SeaWiFS	Oregon State University (OSU)	Net primary productivity (VGPM, EppleyVGPM, CbPM)	Global, 9 km	September 1997 – December 2010; monthly average
MODIS				July 2002 - present; monthly average
VIIRS				2012 - present; monthly average
SMOS	European Space Agency (ESA)	Sea surface salinity	Global, 100km	July 2009- present; monthly average
CCI		Multiple-satellite-merged	Global, 4 km	1997 – 2016;

		chlorophyll concentration		daily average, monthly average
CarbonTracker	National Oceanic and Atmospheric Administration (NOAA)	Atmospheric pCO_2 (after correction of the air pressure, water vapour, and spatial interpolation)	Global, 25 km	2000-2016; daily average, monthly average
Relative Humidity		Relative humidity	Global, 100 km	2000-2016; daily average
AVHRR_OI		Sea surface temperature	Global, 25 km	1981 – present; daily average, monthly average
Underway pCO_2	Carbon Dioxide Information Analysis Center (CDIAC) at the U.S. Department of Energy's Oak Ridge National Laboratory	Sea surface pCO_2, temperature, salinity	underway	1992-2015; underway

References of the self-developed algorithms by SOED:

Please visit www.SatCO2.com for more information.

Appendix 4: Data file naming

The name format of the data file in this system is:

Creator _ Satellite _ Sensor _ Time range _ Level _ Region _ Spatial resolution _ Parameter _ Algorithm/version

Example 1: orbit data

SIO_HY1B_COCTS_20110111003600_L3A_NODEF_1KM_SDD_HE2018

"SIO" means it is produced by the Second Institute of Oceanography of the Ministry of Natural Resources. "HY1B_COCTS" means the raw data came from the COCTS sensor on the HY-1B satellite. The image was photographed at 00:36 am (GMT) on January 11, 2011. Product level is L3A. "NODEF" means the product is single orbit data with varying regions. The spatial resolution is 1 km. Product category is seawater transparency (SDD). "HE2018" means the algorithm is proposed by He et al. (year) and the version is year 2018.

Example 2: daily or monthly data

NASA_SNPP_VIIRS_20130401TO20130430_L3B_GLOBAL_9KM_RRS443_V2017

"NASA" means the data come from NASA. "SNPP_VIIRS" indicates that the original data are from the VIIRS sensor on the SNPP satellite. The imaging time is April 1-30, 2013, and this product is monthly averaged data. Product level is L3B. "GLOBAL" means it covers the globe. The spatial resolution is 9 km. The product category is 443-nm band remote sensing reflectance (RRS443). The data version is year 2017.

The main index fields and their meanings are as follows:

1. Creator

Creator	Full Name
CMEMS	Copernicus marine Environment Monitoring Service
BEC	SMOS Barcelona Expert Center, ESA
ESA	European Space Agency
ESACCI	Climate Change Initiative, European Space Agency
NASA	National Aeronautics and Space Administration, U.S.
NCEP	National Centers for Environmental Prediction, NOAA
NOAA	National Oceanic and Atmospheric Administration, U.S.
OBPG	Ocean Biology Processing Group, NASA
OSU	Organ State University
RSS	Remote Sensing System
SIO	Second Institute of Oceanography, MNR, China

2. Region

Region	Full Name
AER	Asian and Europe Region
BOH	Bohai Sea
CJE	Changjiang River Estuary
EAMS	East Asian Marginal Seas
EAMSL	East Asian Marginal Seas
EIO	East Indian Ocean
GLOBAL	Global oceans
NODEF	Orbit Data
PACIND	Pacific Ocean and Indian Ocean
SCS	South China Sea
WPO	West Pacific Ocean

3. Satellites and sensors

Satellite	Sensor	Full Name/Note
Aqua	MODIS	Moderate Resolution Imaging Spectroradiometer
Aquarius	Aquarius	NASA's 'Salt of the Earth' Aquarius
COMS	GOCI	Communication, Ocean and Meteorological Satellite, Geostationary Ocean Color Imager
GF4	CCD	GaoFen-4, Charge-Coupled Device
HY1B	COCTS	Haiyang-1B, Chinese Ocean Color and Temperature Scanner
MERGE	MERGE	Derived from Multi-satellites/sensors
MODEL	MODEL	Derived from numerical model
MODEL	MERGE	The same as MODEL_MODEL
MODIS	MODIS	The same as Aqua_MODIS
NCEP	MERGE	The same as MODEL_MODEL
NOAA	AVHRR	Advanced Very High-Resolution Radiometer
SAT	MERGE	The same as MERGE_MERGE
SAT	SENSOR	The same as MERGE_MERGE
SeaWiFS	SeaWiFS	Sea-viewing Wide Field-of-view Sensor
SMAP	SMAP	Soil Moisture Active Passive
SMOS	SMOS	Soil Moisture and Ocean Salinity
SMOS	MERGE	The same as SMOS_SMOS
SNPP	VIIRS	Suomi National Polar-orbiting Partnership, Visible and Infrared Imager/Radiometer Suite

4. Product Level

L3A	Single orbit data
L3B	Composite data from multiple orbit data

5. Parameter

Parameter	Full Name	Unit
ACD	Absorption coefficient of the Colored Dissolved Organic Matter and detritus at 443nm	m^{-1}
ACP	Atmospheric pCO2	μatm
CHL	Chlorophyll-a	mg/m3
CP	Coefficient of Attenuation Particle	m^{-1}
CPOM	Coefficient of Attenuation Organic Particle	m^{-1}
DSW	The Total Days of Disastrous wave	count
HUM	Relative Humidity	%
KD3	Diffuse Attenuation Coefficient at 490nm	m^{-1}
LWN412	Normalized Water-Leaving Radiance at 412nm	$mW/cm^2/\mu m/Sr$
LWN443	Normalized Water-Leaving Radiance at 443nm	$mW/cm^2/\mu m/Sr$
LWN490	Normalized Water-Leaving Radiance at 490nm	$mW/cm^2/\mu m/Sr$
LWN519	Normalized Water-Leaving Radiance at 519nm	$mW/cm^2/\mu m/Sr$
LWN520	Normalized Water-Leaving Radiance at 520nm	$mW/cm^2/\mu m/Sr$
LWN550	Normalized Water-Leaving Radiance at 550nm	$mW/cm^2/\mu m/Sr$
LWN565	Normalized Water-Leaving Radiance at 565nm	$mW/cm^2/\mu m/Sr$
LWN628	Normalized Water-Leaving Radiance at 628nm	$mW/cm^2/\mu m/Sr$
LWN670	Normalized Water-Leaving Radiance at 670nm	$mW/cm^2/\mu m/Sr$
LWN769	Normalized Water-Leaving Radiance at 769nm	$mW/cm^2/\mu m/Sr$
MLD	Mixed Layer Thickness/Depth	m
NAP	Non-Algal Particle	m^{-1}
NPP	Net primary Production	mg $C/m^2/day$
PAR	Photosynthetically Active Radiation	Einstein/ m^2/d
PIC	Sea Surface Particle Inorganic Carbon	mol/m^3
POC	Sea Surface Particle Organic Carbon	mg/m^3
PRESS	Mean Sea Level Pressure	Pa

RRS410	Remote Sensing Reflectance at 410nm	sr^{-1}
RRS412	Remote Sensing Reflectance at 412nm	sr^{-1}
RRS443	Remote Sensing Reflectance at 443nm	sr^{-1}
RRS469	Remote Sensing Reflectance at 469nm	sr^{-1}
RRS486	Remote Sensing Reflectance at 486nm	sr^{-1}
RRS488	Remote Sensing Reflectance at 488nm	sr^{-1}
RRS490	Remote Sensing Reflectance at 490nm	sr^{-1}
RRS510	Remote Sensing Reflectance at 510nm	sr^{-1}
RRS531	Remote Sensing Reflectance at 531nm	sr^{-1}
RRS547	Remote Sensing Reflectance at 547nm	sr^{-1}
RRS551	Remote Sensing Reflectance at 551nm	sr^{-1}
RRS555	Remote Sensing Reflectance at 555nm	sr^{-1}
RRS645	Remote Sensing Reflectance at 645nm	sr^{-1}
RRS667	Remote Sensing Reflectance at 667nm	sr^{-1}
RRS670	Remote Sensing Reflectance at 670nm	sr^{-1}
RRS671	Remote Sensing Reflectance at 671nm	sr^{-1}
RRS678	Remote Sensing Reflectance at 678nm	sr^{-1}
SDD	Secchi Disk Depth	m
SLA	Sea Level Anomaly	m
SSC	Suspended Particulate Matter Concentration	mg/L
SSS	Sea Surface Salinity	psu
SST	Sea Surface Temperature	℃
SSW	Sea Surface Wind Field	m/s
SWH	Significant Wave Height	m
TAU	Aerosol Optical Thickness	-
TSM	Total Suspended Matter	mg/L
VIS	Visibility at Sea Surface	km
WCP	Aquatic pCO_2	μatm

Appendix 5： System calculation

S5.1. Spherical coordinate system

SatCO2 platform uses the WGS84 coordinate system. The settings of the geographic coordinate system are as follows:

GEOGCS["WGS 84",

DATUM["WGS_1984",

SPHEROID["WGS 84",6378137,298.257223563,

AUTHORITY["EPSG","7030"]],

TOWGS84[0,0,0,0,0,0,0],

AUTHORITY["EPSG","6326"]],

PRIMEM["Greenwich",0,AUTHORITY["EPSG","8901"]],

UNIT["degree",0.0174532925199433,AUTHORITY["EPSG","9108"]],

AUTHORITY["EPSG","4326"]]

S5.2. Gridding method of in situ data

In general, a series of discrete points in the study area need to be mapped on regular grid for processing, or combined with other gridded data. Creating a raster grid from discrete in situ data points requires the process of interpolation of discrete data. Figure S1 is a schematic diagram of grid interpolation.

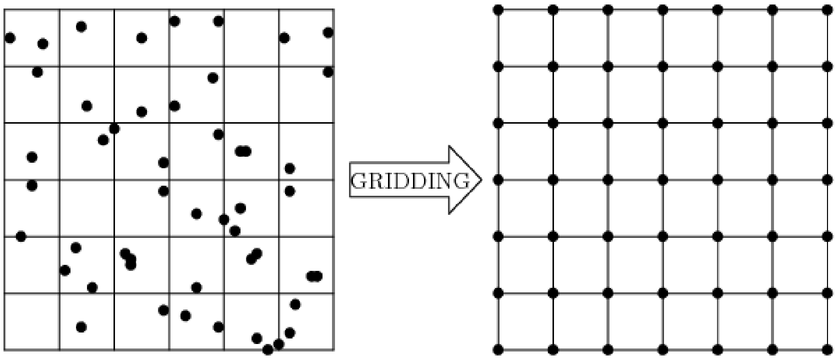

Figure S1. Schematic diagram of gridding interpolation.

The interpolation method in SatCO2 platform is the nearest interpolation method. It is to assign the corresponding in situ data, which are the closest of the space distance to the target raster. The advantage of this method is that the original in situ grid values will not be changed and the processing speed is fast.

S5.3. Spatial-temporal matching

The strategies of spatial-temporal matching processing of in situ data and satellite images in SatCO2 platform are as follows:

1) Take the latitude and longitude data of in situ sampling points, and match the longitude and latitude of satellite data. Due to the large spatial scale of satellite data, there will be multiple sampling points corresponding to the same satellite grid data (for example, within the same 4-km grid).

2) The time information of in situ sampling points corresponds to the time of satellite image. Since satellite data are daily, 10-day average, or monthly average data, there will be one satellite data value, corresponding to multiple sampling points (such as sampling within 10 days or continuous station sampling).

3) If the in situ sampling point cannot match the valid satellite data, the user can choose to match the climatological satellite data.

If multiple satellite images that meet the requirements are matched, a numerical average is taken as the matching result.

Appendix 6：Air-sea CO2 flux calculation

We adopt the commonly used method to calculate the air-sea CO2 flux, which is based on CO_2 partial pressure difference between surface sea water and atmosphere and on CO2 gas transfer velocity. The equation is as follows:

$$\mathrm{Flux} = \Delta p\mathrm{CO2} \times \mathrm{E} = (\mathrm{WCP} - \mathrm{ACP}) \times \mathrm{K_H^{CO2}} \times \rho \times \mathrm{C_2} \times \mathrm{k} \times 24 \times 10^{-2}$$

where,

1）ACP: partial pressure of CO_2 in atmosphere (μatm)

WCP: wpartial pressure of CO_2 in seawater(**μ**atm)

SST: sea surface temperature (°C)

SSS: sea surface salinity (psu)

SSW: sea surface wind speed (m/s)

2）KHCO2 : dissolution efficient of CO_2 (mol kg^{-1} atm^{-1})

$\ln(K_H^{CO2}) = -60.2409 + 93.4517\times(100/T) + 23.3585\times\ln(T/100) + SSS\times[0.023517 - 0.023656\times(T/100) + 0.0047036\times(T/100)^2]$

$T = SST\ (℃) + 273.15$

3）ρ: seawater density, which can be calculated using surface water temperature and salinity (Millero, 2013)(kg m^{-3})

$\rho=(\rho_w+A*S+B*S^{3/2}+C*S^2)*10^{-3}$

$\rho_w=999.842594+6.793952*10^{-2}*SST-9.09529*10^{-3}*SST^2+1.001685*10^{-4}*SST^3-1.120083*10^{-6}*SST^4+6.536332*10^{-9}*SST^5$

$A=0.824493-4.0899*10^{-3}*SST+7.6438*10^{-5}*SST^2-8.2467*10^{-7}*SST^3+5.3875*10^{-9}*SST^4$

$B=-5.72466*10^{-3}+1.0227*10^{-4}*SST-1.6546*10^{-6}*SST^2$

$C=4.8314*10^{-4}$

4）C2: wind speed coefficient, which has been calculated and uploaded in the SOED database.

To calculate monthly average flux, it is often necessary to consider the influence of high-frequency wind speed change (e.g., daily) on the monthly average wind speed, using the coefficient of C2 (Wanninkhof, 2002).The C2 coefficient is not needed when calculating daily flux.

$$C_2 = \frac{(U_j^2)_{mean}}{(U_{mean})^2}$$

U_j is high-frequency satellite-derived wind speed (e.g., daily), and U_{mean} is satellite-derived monthly average wind speed, both units being m s^{-1}.

5）k: gas transfer velocity (cm ħ$^{-1}$)

Based on the relationship between gas transfer velocity (k) and wind speed at 10 m above sea level (U_{10}), the commonly used equations for k are shown in table below.

No.	Equation	References
1	$k_{660} = 0.31 \times u_{10}^2$ (Instantaneous wind speed) $k_{660} = 0.39 \times u_{10}^2$ (Long-term average wind speed)	Wanninkhof (1992)(Instantaneous) Wanninkhof (1992)(Long-term)
2	$k_{660} = 0.27 \times u_{10}^2$	Sweeney et al. (2007)
3	$k_{600} = 0.266 \times u_{10}^2$	Ho et al. (2006)
4	$k_{660} = 0.24 \times u_{10}^2$	Wanninkhof et al. (2009)
5	$k_{600} = 0.17 \times u_{10}$ (u_{10}< 3.6 m/s)	Liss and Merlivat (1986)
6	$k_{660} = 0.0283 \times u_{10}^3$	Wanninkhof and McGillis (1999)
7	$k_{600} = 2.85 \times u_{10}$ -9.65 (3.6 < u_{10}< 13 m/s)	Liss and Merlivat (1986)
8	$k_{600} = 5.9 \times u_{10}$ -49.3 (u_{10}> 13 m/s)	Liss and Merlivat (1986)

k_{660} and k_{600} mean the k with the the Schmidt number (Sc) of 660 and 600, respectively.

$k = k_{600} \times (Sc/600)^{-0.5}$ and $k = k_{660} \times (Sc/660)^{-0.5}$

When sea suface temperature (SST) ranges 0-30 °C, the Sc can be calculated with the following equation (Wanninkhof, 1992),

$Sc = 2073.1 - 125.62 \times sst + 3.6276 \times sst^2 - 0.043219 \times sst^3$

where sst is sea suface temperature, with the units of °C.

For the calculation of satellite-derived air-sea CO2 flux in the open ocean, the k-u_{10} equation of #1 (long-term wind speed) and #2 in the above table are commonly used.

References

[1] Bai, Y., Cai, W.-J., He, X., Zhai, W., Pan, D., Dai, M., Yu, P., 2015. A mechanistic semi‐analytical method for remotely sensing sea surface pCO2 in river‐dominated coastal oceans: A case study from the East China Sea. Journal of Geophysical Research : Oceans, 120, doi:10.1002/2014JC010632.

[2] Song, X., Bai, Y., Cai, W.-J., Chen, C.-T. A., Pan, D., He, X., Zhu Q., 2016, Remote Sensing of Sea Surface pCO2 in the Bering Sea in Summer Based on a Mechanistic Semi-Analytical Algorithm (MeSAA), Remote Sensing, 8, 558; doi:10.3390/rs8070558 .

[3] Ho, D.T., Law, C.S., Smith, M.J., Schlosser, P., Harvey, M., Hill, P., 2006. Measurements of air-sea gas exchange at high wind speeds in the Southern Ocean: Implications for global parameterizations. Geophysical Research Letters, 33(16): L16611, doi:10.1029/2006GL026817.

[4] Liss, P.S. and Merlivat, L., 1986. Air-sea gas exchange rates: introduction and synthesis. In: P. Buat-Menard (Editor), The Role of Air-Sea Exchange in Geochemical Cycling. Reidel, Hingham, MA, pp. 113-129.

[5] Millero, 2013, Chemical Oceanography (4th Edition), CRC Press, Taylor & Francis Group, International Standard Book Number-13: 978-1-4665-1255-9 (eBook - PDF).

[6] Sweeney, C., Gloor, E., Jacobson, A. R., Key, R. M., McKinley, G., Sarmiento, J. L., Wanninkhof, R., 2007. Constraining global air-sea gas exchange for CO2 with recent bomb C-14 measurements. Global Biogeochemical Cycles, 21(2): GB2015, doi:10.1029/2006GB002784.

[7] Wanninkhof, R., 1992. Relationship between wind speed and gas exchange over the ocean. Journal of Geophysical Research, 97(C05): 7373-7382.

[8] Wanninkhof, R., Asher, W.E., Ho, D.T., Sweeney, C. and McGillis, W.R., 2009. Advances in quantifying air-sea gas exchange and environmental forcing, Annual Review of Marine Science. Annual Review of Marine Science, pp. 213-244.

[9] Wanninkhof, R., Doney, S. C., Takahashi, T., and McGillis, W.: The effect of using time-averaged winds on regional air-sea CO2 fluxes, in: Gas Transfer at Water Surfaces, edited by: Donelan, M., Geophys. Monogr. Ser., Amrican Geophysical Union,Washington, D.C., 127, doi:10.1029/GM127p0351, 351–357, 2002.

[10] Weiss, E.F. and Price, R.A., 1980. Nitrous oxide solubility in water and sea water. Marine Chemistry, 8: 347-359.

Appendix 7：Algorithms for HAB detection

A rapid increase in the number of microalgae is considered as an algal bloom. Harmful algal bloom (HAB) is a bloom that results in negative impact on plants and animals. Over the past decade, significant achievements were made to synoptically detect and characterize the location and extent of HABs using ocean color satellite sensors. A lot of greatly improved algorithms have been developed to more accurately retrieve phytoplankton proxies in coastal waters. Therefore, the SatCO2 software includes five HAB detection modules, which have been successfully tested in some typical coastal regions such as the East China Sea, the Gulf of Mexico, and so on. Detailed descriptions of these modules are as follows.

S7.1. The HAB algorithm in the East China Sea

This module integrates two HAB algorithms in the East China Sea. The first algorithm is a multispectral approach for discriminating *P. donghaiense* blooms from other water types based on MODIS R_{rs} spectral shape discrimination. Its procedure involves two steps. First, the bloom waters are identified by the lowRrs(555) and high RAB (Algal bloom ratio). Second, two new indices of *P. donghaiense* index (PDI) and diatom index (DI) are developed for discriminating *P. donghaiense* from diatom blooms. The second algorithm is a VIIRS-based approach for detecting HAB. Detailed method is schematically illustrated in Figure S2.

（1）MODIS HAB algorithm description：

Algal bloom ratio (R_{AB}) is defined by

$$\mathrm{R}_{AB}=\frac{R_{rs}(555)}{R_{rs}(531)}$$

P. donghaiense index（PDI）:

$$PDI=\frac{R_{rs}\_\mathrm{slope}(555,531)-R_{rs}\_\mathrm{slope}(531,488)}{R_{rs}(555)-R_{rs}(488)}$$

where

$$R_{rs}\_\mathrm{slope}(\lambda_1,\lambda_2)=\frac{R_{rs}(\lambda_1)-R_{rs}(\lambda_2)}{\lambda_1-\lambda_2}$$

Diatom index（DI）:

$$DI=\frac{R_{rs}(645)-\left[R_{rs}(555)+\frac{555-645}{555-667}\left(R_{rs}(667)-R_{rs}(555)\right)\right]}{R_{rs}(645)}$$

（2）VIIRS HAB algorithm description

Algal bloom ratio (R_{AB}) is defined by

$$R_{AB}=\frac{R_{rs}(551)}{R_{rs}(486)}$$

Bloom index (BI) is defined by

$$BI=\frac{\left[R_{rs}(443)+\frac{486-443}{551-443}\left(R_{rs}(551)-R_{rs}(443)\right)\right]-R_{rs}(486)}{\left(R_{rs}(551)-R_{rs}(443)\right)}$$

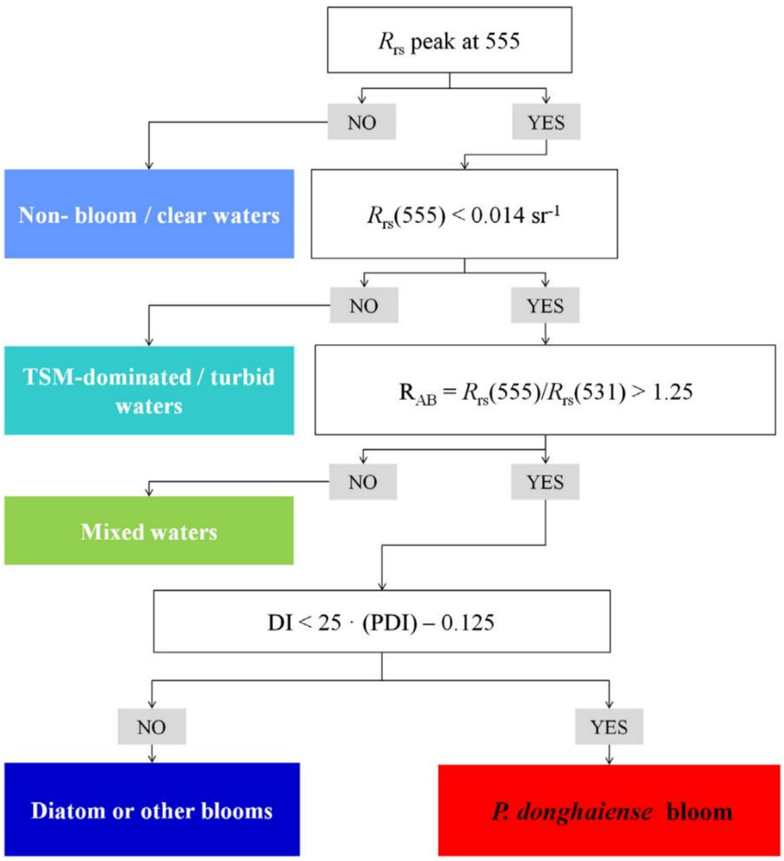

Figure S2. Schematic procedure of MODIS multispectral method for the identification of *P. donghaiense*.

S7.2. RBD-based HAB algorithm

This module introduces the technique developed by Amin et al. (2009) primarily for detecting *Karenia brevis* (*K. brevis*) blooms throughout the Gulf of Mexico. This detection technique for blooms with low backscatter, which is named the Red Band Difference (RBD) technique here. These techniques take advantage of the relatively high solar-induced chlorophyll fluorescence and low backscattering of *K. brevis* blooms. The techniques are applied to the detection and classification of K. brevis blooms from Moderate Resolution Imaging Spectroradiometer (MODIS) ocean color measurements.

（1）MODIS RBD algorithm description：

Red Band Difference (*RBD*) is defined by

$$RBD = nLw(678) - nLw(667)$$

Threshold of algal bloom waters:

$$RBD > 0.15\mathrm{W/m^2/\mu m/sr}$$

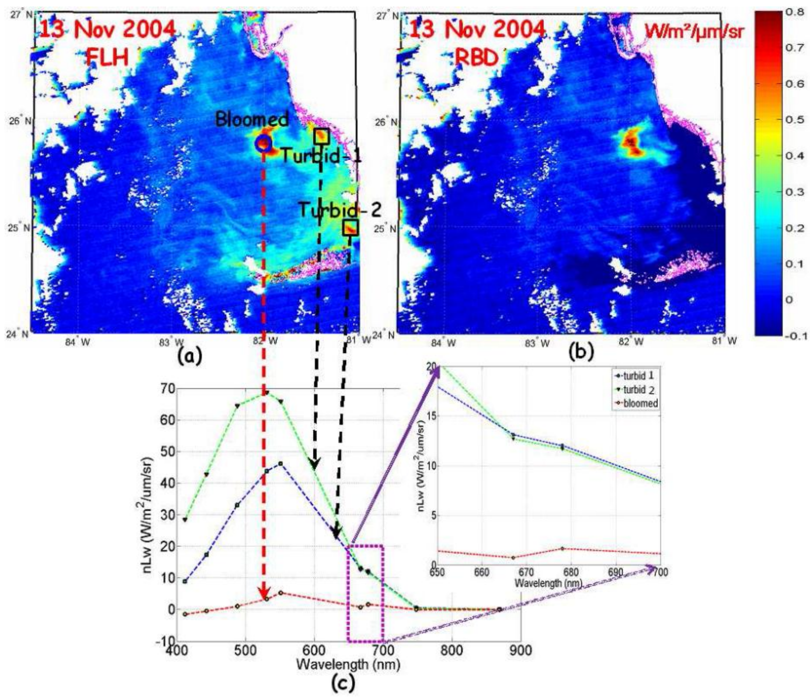

Figure S3. MODIS (Aqua) bloom image from November, 13 2004 for the WFS (a) FLH (W/m^2/μm/sr) image, (b) RBD (W/m^2/μm/sr) image, and (c) Normalized water-leaving radiance spectra taken from the bloomed and turbid waters indicated by “circle” and “squares,” respectively, in the FLH image.

S7.3. RGCI-based HAB algorithm

This module integrates a novel empirical Chla algorithm based on a Red-Green-Chorophyll-Index (RGCI), which was developed by Le et al. (2013), and validated for MODIS and VIIRS observations. The algorithm showed robust performances in coastal waters such as Tampa Bay and the northeastern Gulf of Mexico. Oi et al. (2015) used RGCI from VIIRS to observe *Karenia brevis* blooms in the northeastern Gulf of Mexico, which can overcome deficiency rising from the absence of a fluorescence band.

（1）MODIS RGCI algorithm description：

Red-Green-Chorophyll-Index (*RGCI*) is defined by

$$RGCI = R_{rs}(667)/\ R_{rs}\ (547)$$

The empirical Chla algorithm:

$$\text{Chla} = 0.86 * \exp(5.1 * \text{RGCI})$$

（2）VIIRS RGCI algorithm description：

Red-Green-Chorophyll-Index (*RGCI*) is defined by

$$RGCI = R_{rs}(672)/\ R_{rs}\ (551)$$

The empirical Chla algorithm:

$$\text{Chla} = 0.10 * \exp(11.8 * RGCI)$$

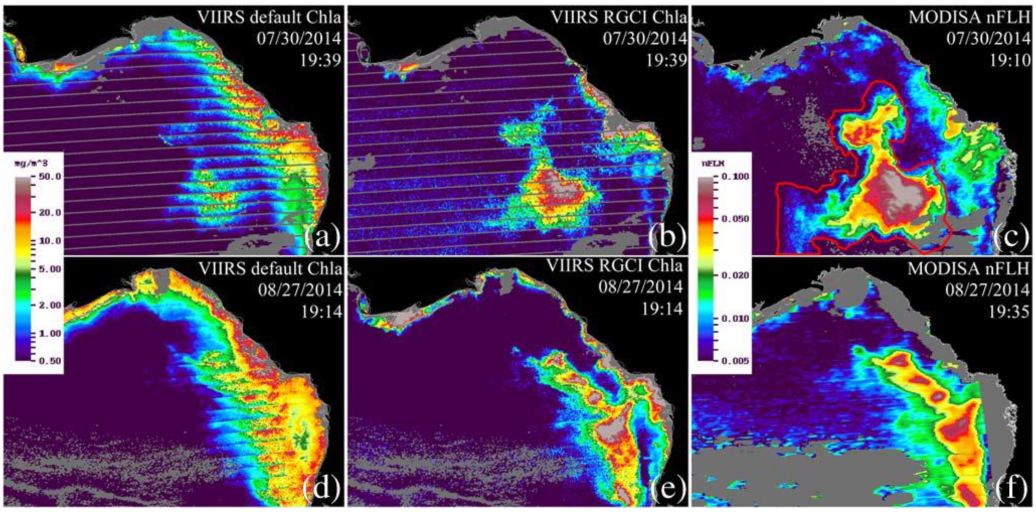

Figure S4. Comparison between (a and d) VIIRS OC3 Chla (mg m^{-3}), (b and e) VIIRS RGCI Chla (mg m^{-3}), and (c and f) MODISA nFLH (mW cm^{-2} μm^{-1} sr^{-1}) for July 30, 2014 (a–c), and August 27, 2014 (d–f). The annotate times are GMT hours and minutes. Black is land, and gray represents clouds or invalid data.

S7.4. ABI-based HAB algorithm

This module integrates new bio-optical algorithm that was developed by Shanmugam et al. (2011), to provide accurate assessments of chlorophyll a (Chl a) concentration for detection and mapping of algal blooms using satellite data in optically complex waters, where the presence of suspended sediments and dissolved substances can interfere with phytoplankton signals and thus confound conventional band ratio algorithms. This algorithm uses normalized water−leaving radiance ratio along with an algal bloom index (ABI) between three visible bands to determine Chl a concentration, which is derived using the Moderate Resolution Imaging Spectroradiometer (MODIS) data and could be extensively used for quantitative and operational monitoring of algal blooms in various regional and global waters.

（1）MODIS ABI algorithm description：

Algal bloom index (*ABI*) is defined by

$$X = ABI = 10^{\left[\left(\frac{nL_W(490)}{nL_W(555)}\right)-\left(\frac{nL_W(443)}{\alpha}\right)\right]/\left[\left(\frac{nL_W(490)}{nL_W(555)}\right)+\left(\frac{nL_W(443)}{\alpha}\right)\right]}$$

$$\left.\begin{array}{c} \aleph = X \times X' \\ X' = \left(\frac{(nL_w(443)\times nL_w(490)/nL_w(555))^2}{(\lambda_{490}-\lambda_{443})}\right) \end{array}\right\}$$

The empirical Chla algorithm:

$$\varepsilon_{chl-a} = 0.1403 \times (\aleph)^{(-0.572)}$$

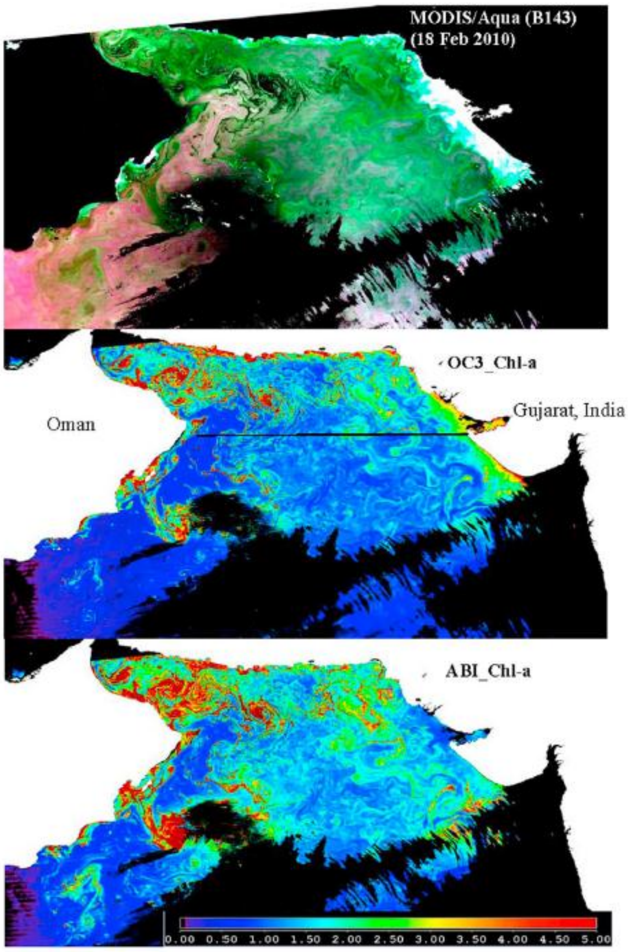

Figure S5. (Top) A MODIS/Aqua true color composite on February 18, 2010 in the Arabian Sea and Gulf of Oman. The corresponding Chl a images derived using (middle) the OC3 and (bottom) ABI algorithms. The combined SeaDAS algorithm and CCS scheme was used for atmospheric correction of MODIS/Aqua data.

S7.5. FLH based HAB algorithm

This module integrates a MODIS fluorescence line height (FLH) based algorithm developed by Hu et al. (2005) to detect and trace harmful algal bloom (HAB), or red tide, in SW Florida coastal waters. Because MODIS fluorescence line height (FLH in W/m^2/μm/sr) data showed the highest correlation with near-concurrent in situ chlorophyll-a concentration (Chl in mg m^{-3}), the results show that the MODIS FLH data provide an unprecedented tool for research and managers to study and monitor algal blooms in coastal environment.

（1）MODIS FLH based Chla algorithm description：

The FLH based Chla algorithm:

$$Chl=1.255 * (FLH * 10)^{0.86}$$

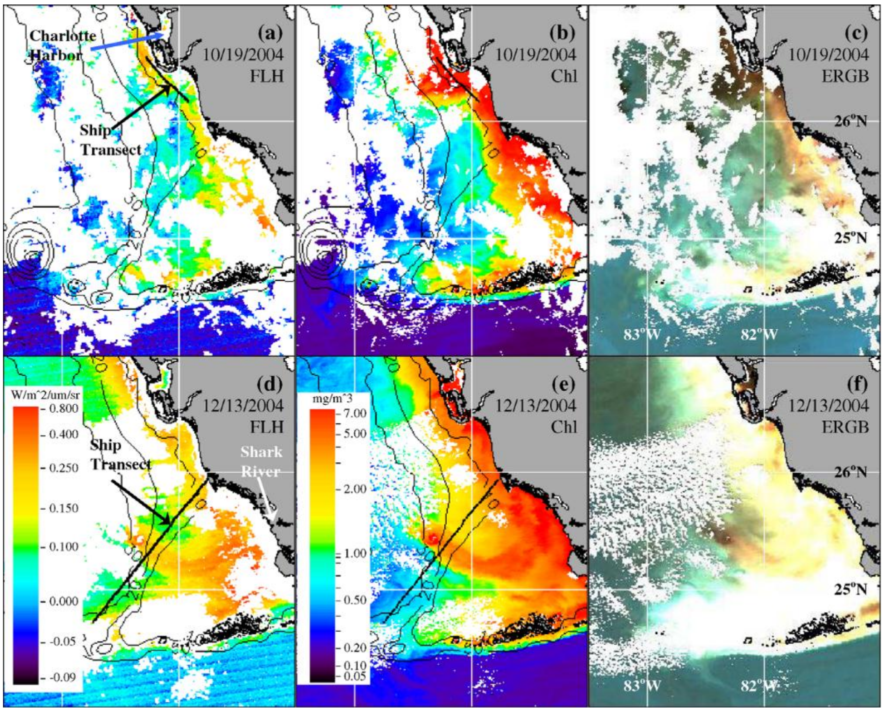

Figure S6. MODIS/Aqua imagery for SW Florida coastal waters. Left column: Fluorescence line height (FLH; W/m^2/μm/sr). The color scale includes negative values. Middle column: Band-ratio chlorophyll concentration (OC3M Chl; mg m^{-3}). Right column: Enhanced RGB (ERGB) composite images from water-leaving radiance in three MODIS wavelengths: 551 nm (R), 488 nm (G), and 443 nm (B).

References:

[1] Tao Bangyi, Mao Zhihua, Lei Hui, et al. A semianalytical MERIS green-red band algorithm for identifying phytoplankton bloom types in the East China Sea[J]. Journal of Geophysical Research: Oceans, 2017,122(3):1772-1788.

[2] Tao Bangyi, Mao Zhihua, Lei Hui, Pan Delu, ShenYuzhang, Bai Yan, Zhu Qiankun, Li Zhien, A novel method for discriminating *Prorocentrum donghaiense* from diatom blooms in the East China Sea using MODIS measurements[J]. Remote Sensing of Environment, 2015,158(0):267-280.

[3] Tao Bangyi, Mao Zhihua, Pan Delu, ShenYuzhang, Zhu Qiankun, Chen Jianyu, Influence of bio-optical parameter variability on the reflectance peak position in the red band of algal bloom waters[J]. Ecological Informatics, 2013,16(0):17-24.

[4] Tao Bangyi, Mao Zhihua, Pan Delu, ShenYuzhang, Optical detection of *Prorocentrum donghaiense* blooms based on multispectral reflectances[J]. Acta Oceanologica Sinica. 2013,32(10):48-56.

[5] Ruhul Amin, Jing Zhou, Alex Gilerson, et al. Novel optical techniques for detecting and classifying toxic dinoflagellate Karenia brevis blooms using satellite imagery [J]. Optics Express, 2009,17(11): 9126.

[6] Chengfeng Le, Chuanmin Hu, David English, et al. Climate-driven chlorophyll-a changes in a turbid estuary: Observations from satellites and implications for management [J]. Remote Sensing of Environment, 2013,130: 11-24.

[7] Lin Qi, Chuanmin Hu, Jennifer Cannizzaro, et al. VIIRS Observations of a Karenia brevis Bloom in the Northeastern Gulf of Mexico in the Absence of a Fluorescence Band [J]. IEEE GEOSCIENCE AND REMOTE SENSING LETTERS, 2015,12(11): 2213-2217.

[8] Palanisamy Shanmugam. A new bio-optical algorithm for the remote sensing of algal blooms in complex ocean waters [J]. JOURNAL OF GEOPHYSICAL RESEARCH, 2011, 116:C04016.

[9] Chuanmin Hu, Frank E. Muller-Karger, Charles (Judd) Taylor et al. Red tide detection and tracing using MODIS fluorescence data: A regional example in SW Florida coastal waters [J]. Remote Sensing of Environment, 2005, 97:311-321.

SECOND INSTITUTE OF OCEANOGRAPHY,MNR 36 Baochubei Road,Hangzhou,China,310012
Tel:86-571-81963112 E-mail:satco2@sio.org.cn URL:www.SatCO2.com